In-line Processing in Scanning Atmospheric Radar Networks

V. Chandrasekar
Colorado State University

Radar Network System

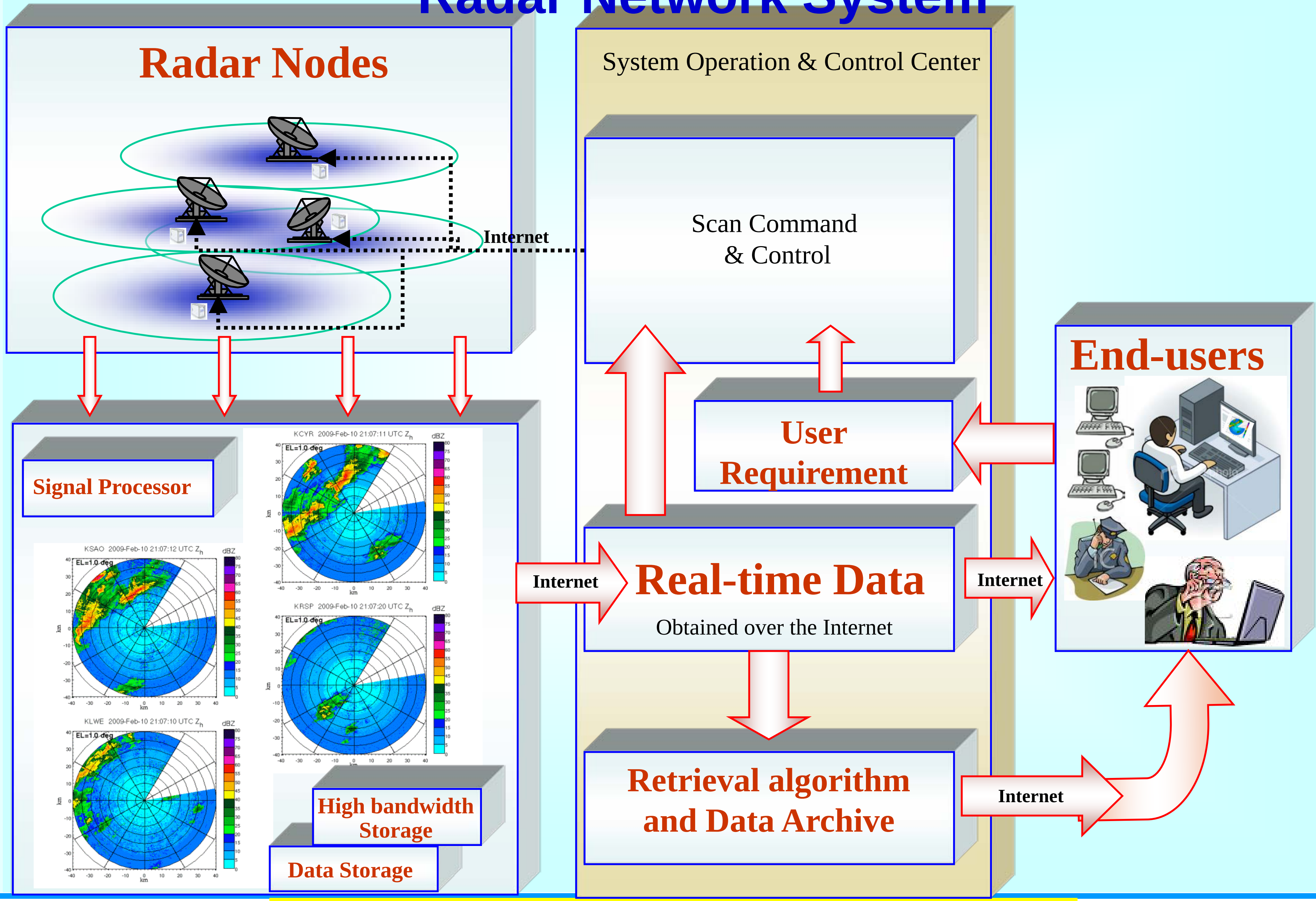

Real time processing of Radar parameter computation

- Radar Variables
- Ground Clutter Filtering
- Range-Velocity Ambiguity Mitigation
- Overlaid Echo Suppression

Estimates of Spectral Moment

❖ The mean received power provides the intensity of precipitation within the resolution volume

$$time\ domain: \hat{P}_h = \frac{1}{N}\sum_{k=0}^{N-1}|v_h[k]|^2 \qquad spectral\ domain: \hat{P}_h = \frac{1}{N^2}\sum_{k=0}^{N-1}|s_h[k]|^2$$

❖ The mean radial velocity of the precipitation is obtained based on the Doppler phase shift (caused by the motion of particles) of the received signal

$$\hat{R}(1) = \frac{1}{N}\sum_{k=0}^{N-2} v_h(k+1)v_h^*(k)$$

$$time\ domain: \hat{\bar{v}} = -\frac{\lambda}{4\pi T_s}\arctan\{\hat{R}(1)\}$$

$$spectral\ domain: \hat{\bar{v}} = \frac{\sum_{k=0}^{N-1} v[k]|s[k]|^2}{\sum_{k=0}^{N-1}|s[k]|^2}$$

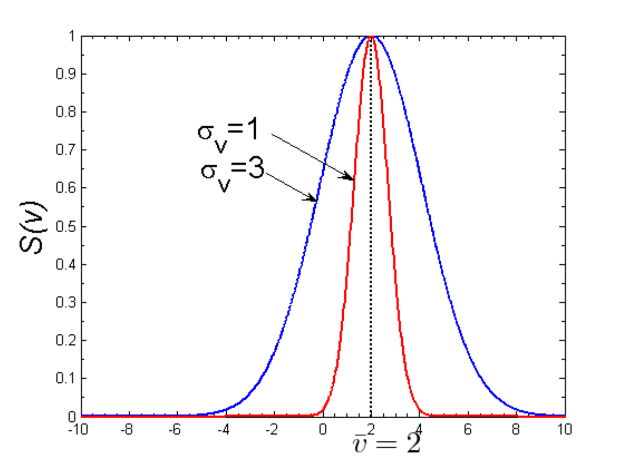

❖ The precipitating volume consist of a large number of hydrometeors with widely varying radial velocities resulting a Doppler velocity spread about the mean velocity. The spectral width gives a measure of turbulence of the medium

$$time\ domain: \hat{\sigma}_v = \frac{\lambda}{2\pi T_s\sqrt{2}}\sqrt{\ln\left|\frac{R(0)}{R(1)}\right|} \qquad spectral\ domain: \hat{\sigma}_v = \sqrt{\frac{\sum_{k=0}^{N-1}(v_k - \hat{\bar{v}})^2|s_k|^2}{\sum_{k=0}^{N-1}|s_k|^2}}$$

Estimates of Polarimetric Variables

❖ Differential reflectivity between polarization channels provides a measure of mean particle shape

$$\hat{Z}_{dr} = 10\log_{10}\left(\frac{\hat{P}_h}{\hat{P}_v}\right)$$

❖ The differential propagation phase shift is the phase difference between vertical polarization and horizontal polarization as the wave propagates through rain

$$time\ domain: \hat{\psi}_{dp} = \arctan\left\{\sum_{k=0}^{N-1} v_v[k]\, v_h^*[k]\right\}$$

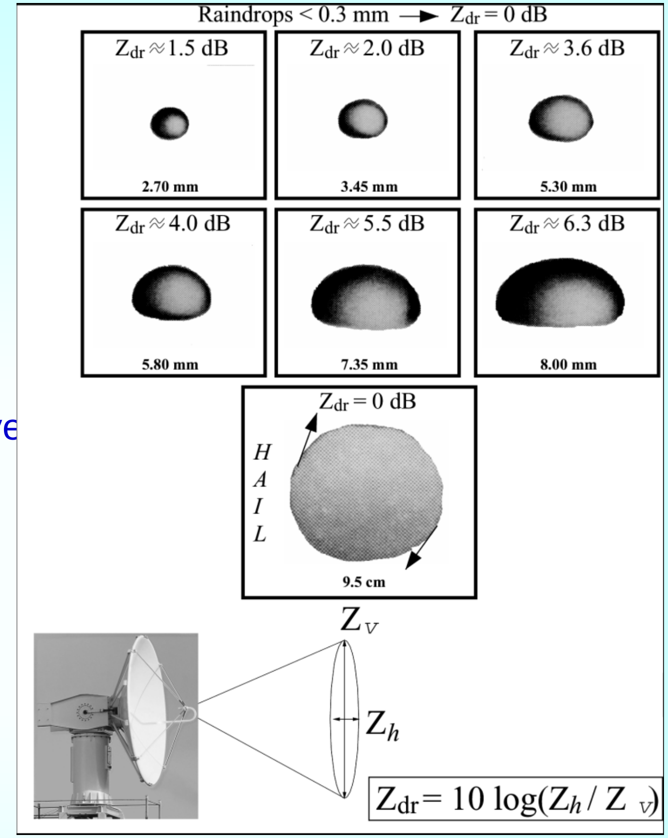

❖ The correlation between the received signal in the horizontal polarization and vertical polarization is gives an indication of similarity in the nature of back scattering from the hydrometeors

$$time\ domain: |\hat{\rho}_{hv}(0)| = \frac{\left|\sum_{k=0}^{N-1} v_v[k]\, v_h^*[k]\right|}{\sqrt{\sum_{k=0}^{N-1} |v_h[k]|^2 \sum_{k=0}^{N-1} |v_v[k]|^2}}$$

$$spectral\ domain: |\hat{\rho}_{hv}(0)| = \frac{\left|\sum_{k=0}^{N-1} s_v[k]\, s_h^*[k]\right|}{\sqrt{\sum_{k=0}^{N-1} |s_h[k]|^2 \sum_{k=0}^{N-1} |s_v[k]|^2}}$$

Spectral Clutter Filtering Example

❖ Obtain spectral coefficients and power spectral density of received signal

$$\mathbf{S}(\mathbf{v},\theta) = \frac{p_c}{\sqrt{2\pi\sigma_c^2}}\exp\left\{-\frac{\mathbf{v}^2}{2\sigma_c^2}\right\} + \frac{p}{\sqrt{2\pi w^2}}\exp\left\{-\frac{(\mathbf{v}-v)^2}{2w^2}\right\} + \frac{2T_s}{\lambda}p_n$$

❖ Obtain adaptive noise floor by sorting spectral coefficients by power

❖ Design notch filter in spectral domain

➢ Estimate clutter model based on Gaussian model fit to zero Doppler region

➢ Estimate notch width based on clutter model and noise

$$n = \left\lfloor \frac{4\sigma_c T_s}{\lambda}\sqrt{2\ln\left[\sqrt{2\pi}\sigma_c\left(\frac{p_c}{\bar{p}_n}\right)\right]}\right\rfloor$$

❖ Notch the clutter signal with a spectral clipper

❖ Interpolate the notch filtered region by iteratively fitting a Gaussian model to the weather signal

❖ Replace the clutter region with model and subtract noise power

Ground Clutter Filtering

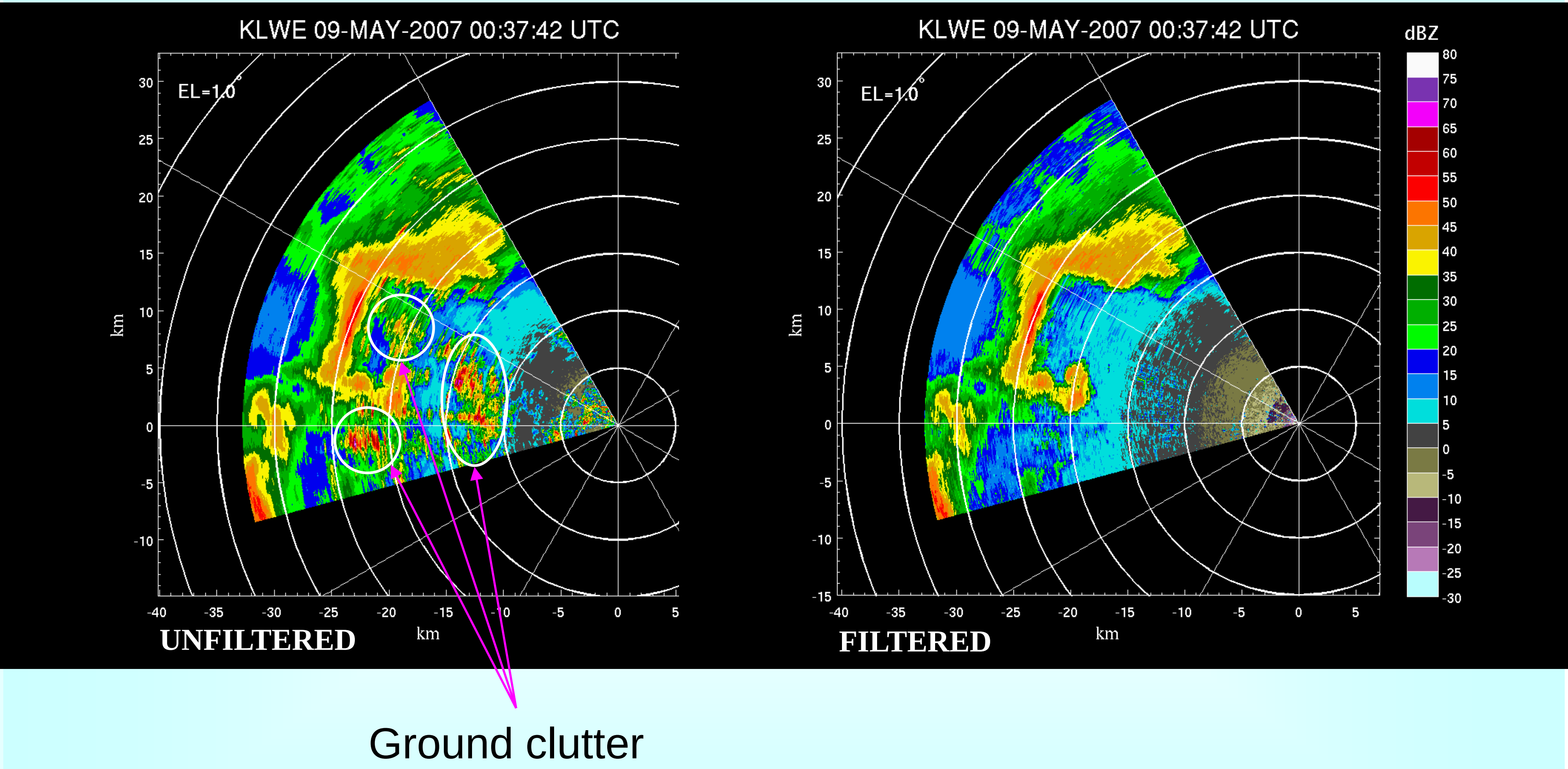

Reflectivity before and after ground clutter filtering. Data collected on May 09, 2007 at Lawton (EL=1 deg).

Ground Clutter Filtering

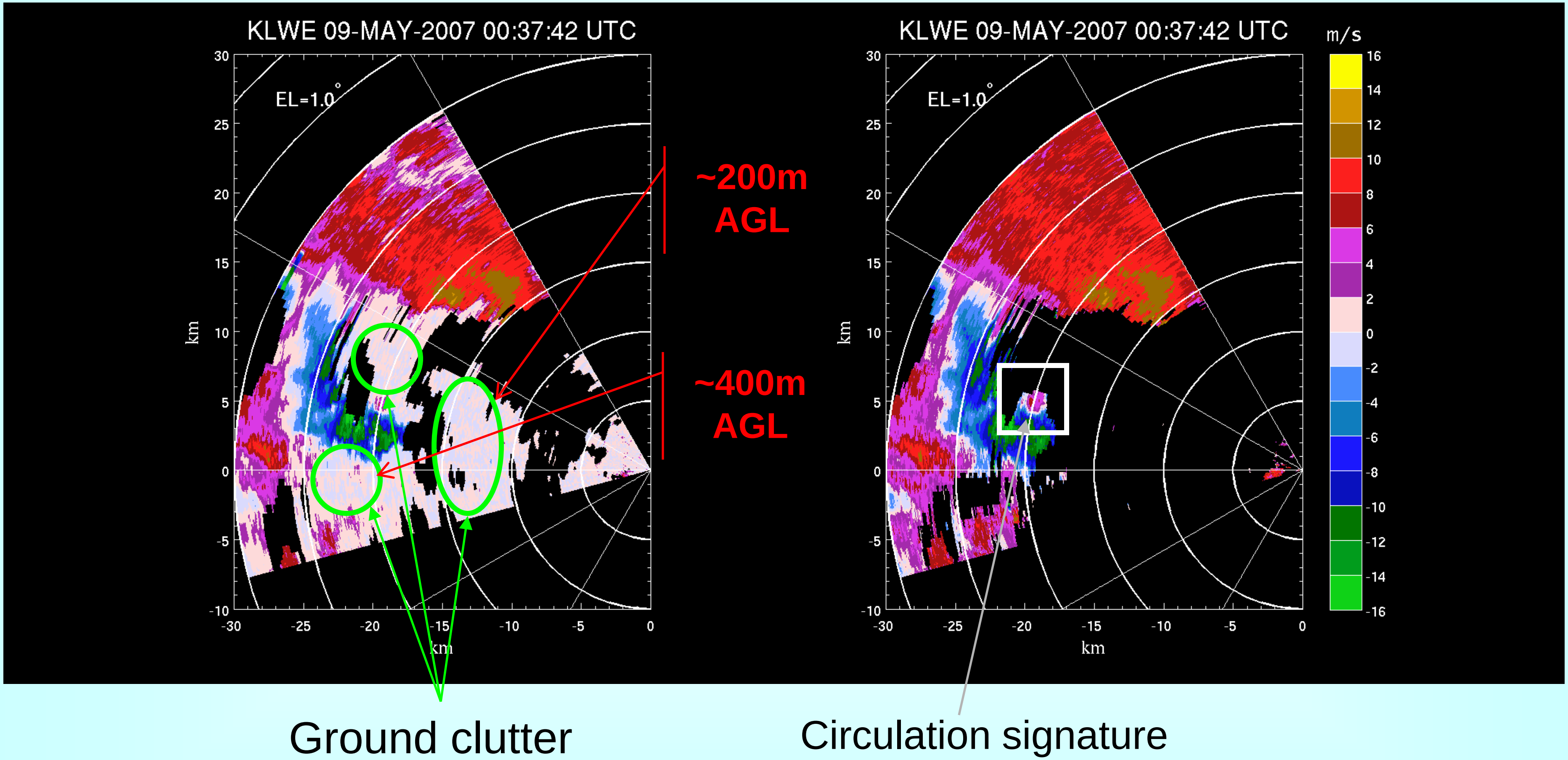

Velocity before and after ground clutter filtering.
Data collected on May 09, 2007 at Lawton (EL=1 deg).

Range-velocity Ambiguity Mitigation Methods

- The maximum unambiguous range and unambiguous velocity have a limitation based on wavelength and pulse repetition time

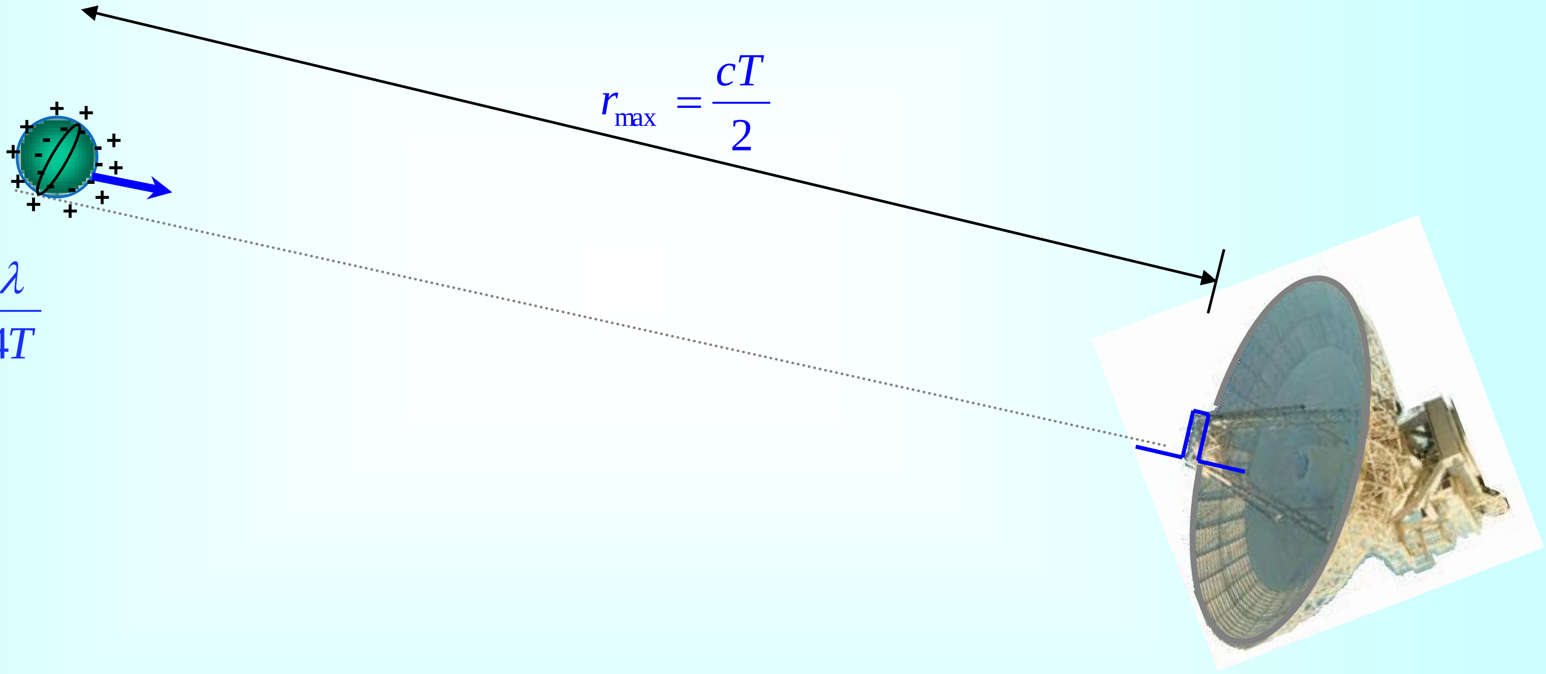

$$r_{max} = \frac{cT}{2}$$

$$v_{max} = \frac{\lambda}{4T}$$

- Maximum unambiguous range and unambiguous velocity are related to each other as

$$r_{max} v_{max} = \frac{c\lambda}{8}$$

Range-velocity Ambiguity Mitigation Methods

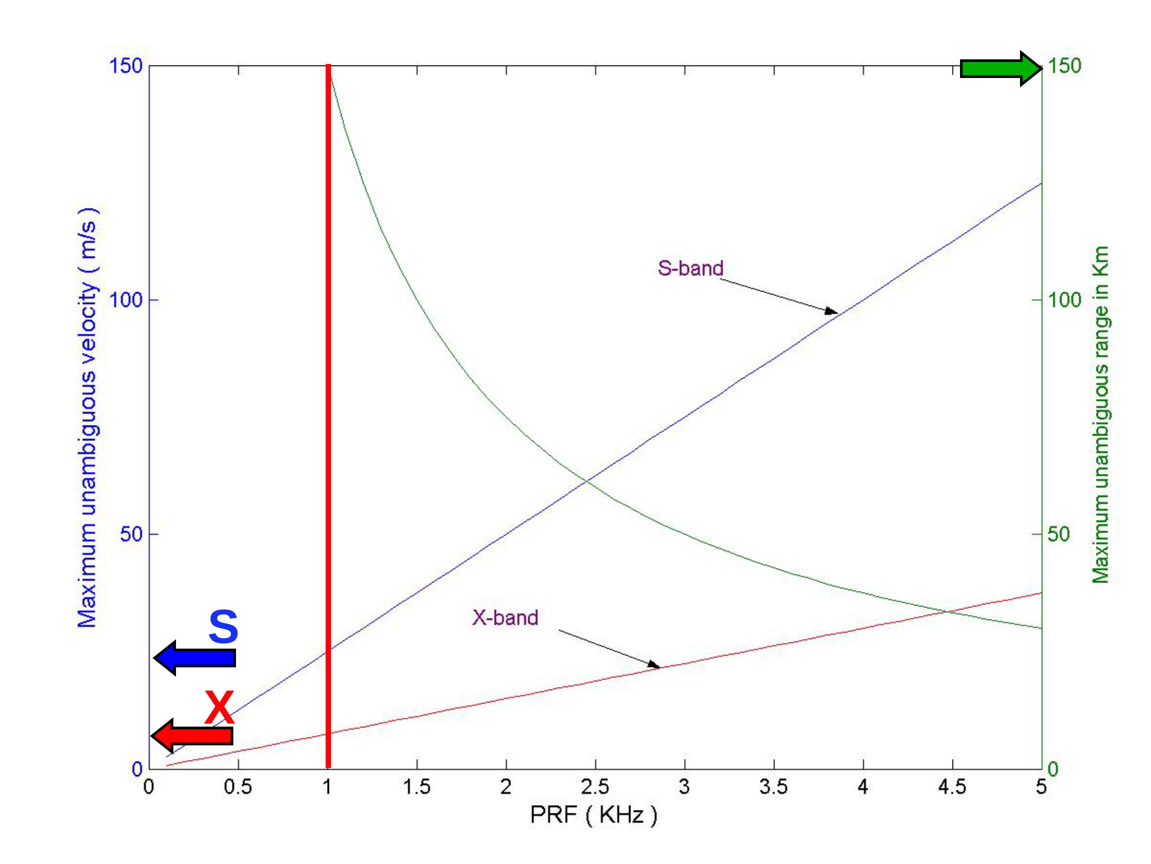

- If v_{max} is increased then r_{max} decreases correspondingly (Range-velocity ambiguity)
- Fundamental limitation of pulsed Doppler radar transmitting uniformly spaced pulses

Radial Velocity Folding in Severe Weather

Velocity measurements with uniform PRT and staggered PRT with CSU-CHILL 2006-Dec-20

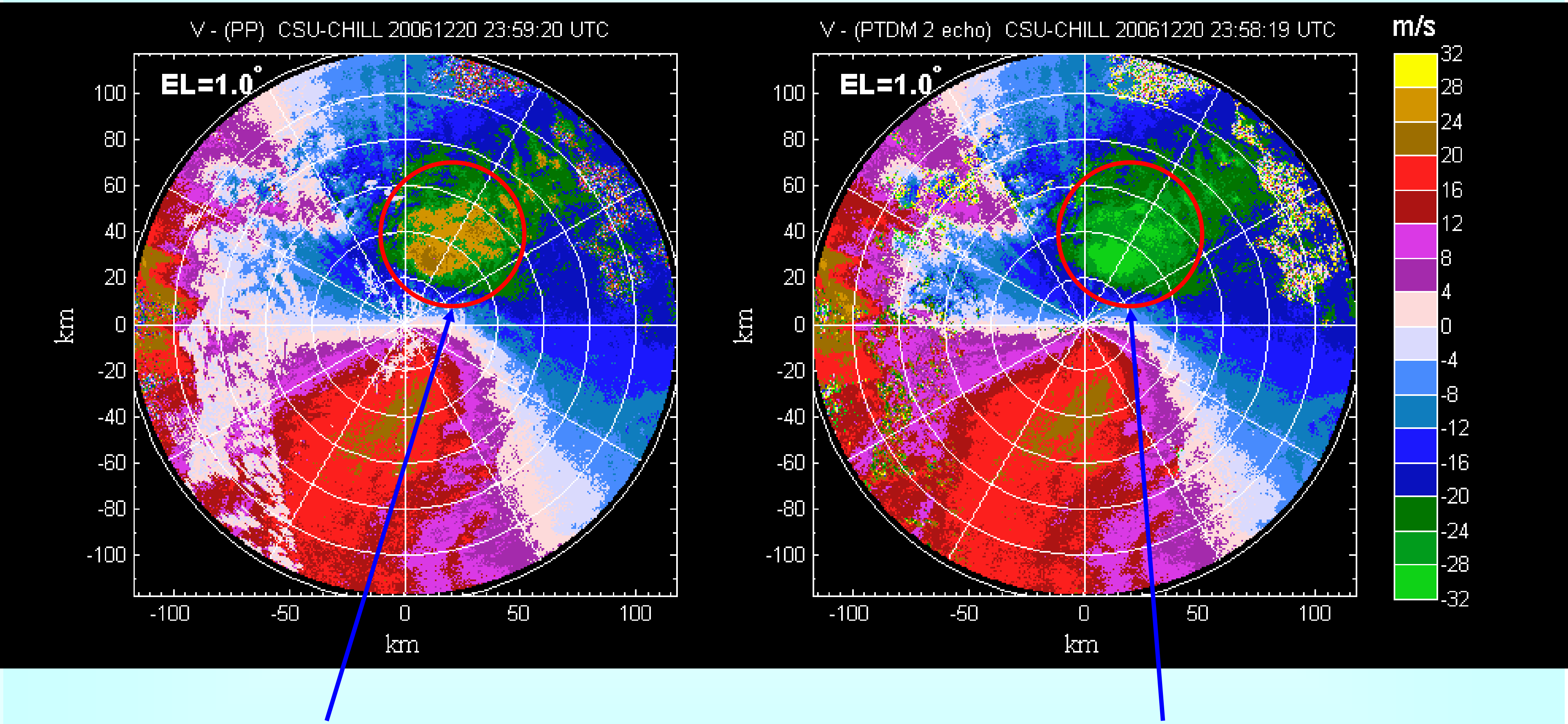

Velocity folding from -27 m/s to 27 m/s

Unfolded velocity folding using staggered PRT waveform

Range-velocity Ambiguity Mitigation Methods

- Phase coding to mitigate range ambiguity
  - Random phase coding
  - Systematic phase coding

- Staggered pulsing to mitigate
  - Staggered PRT
  - Staggered PRF

- Polarization diversity to mitigate range ambiguity

Range-overlay due to shorter PRT

- In order to obtain reasonable unambiguous velocities the Doppler radar's PRT is significantly shorter

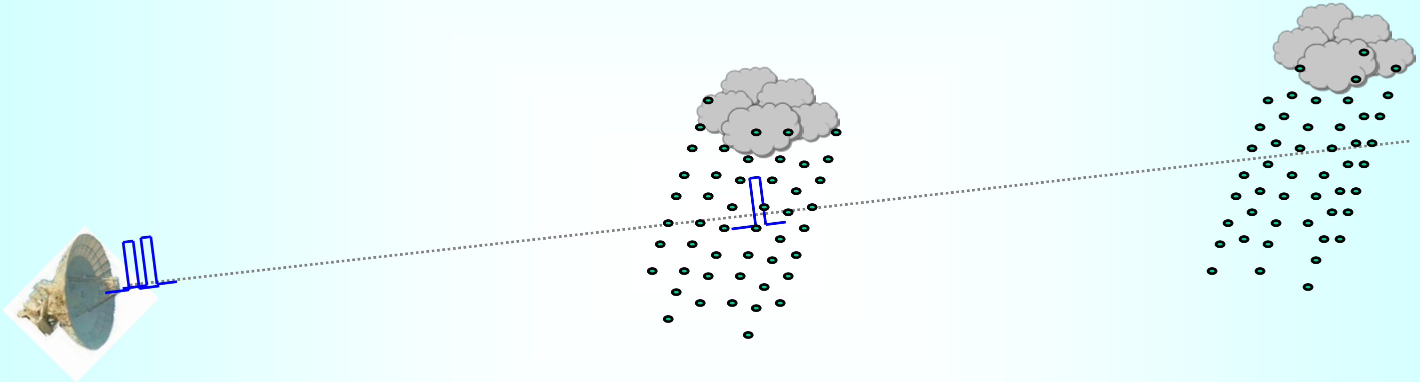

- The shorter PRTs results in range-overlaid echoes which gives erroneous measurements of the Doppler spectral moments

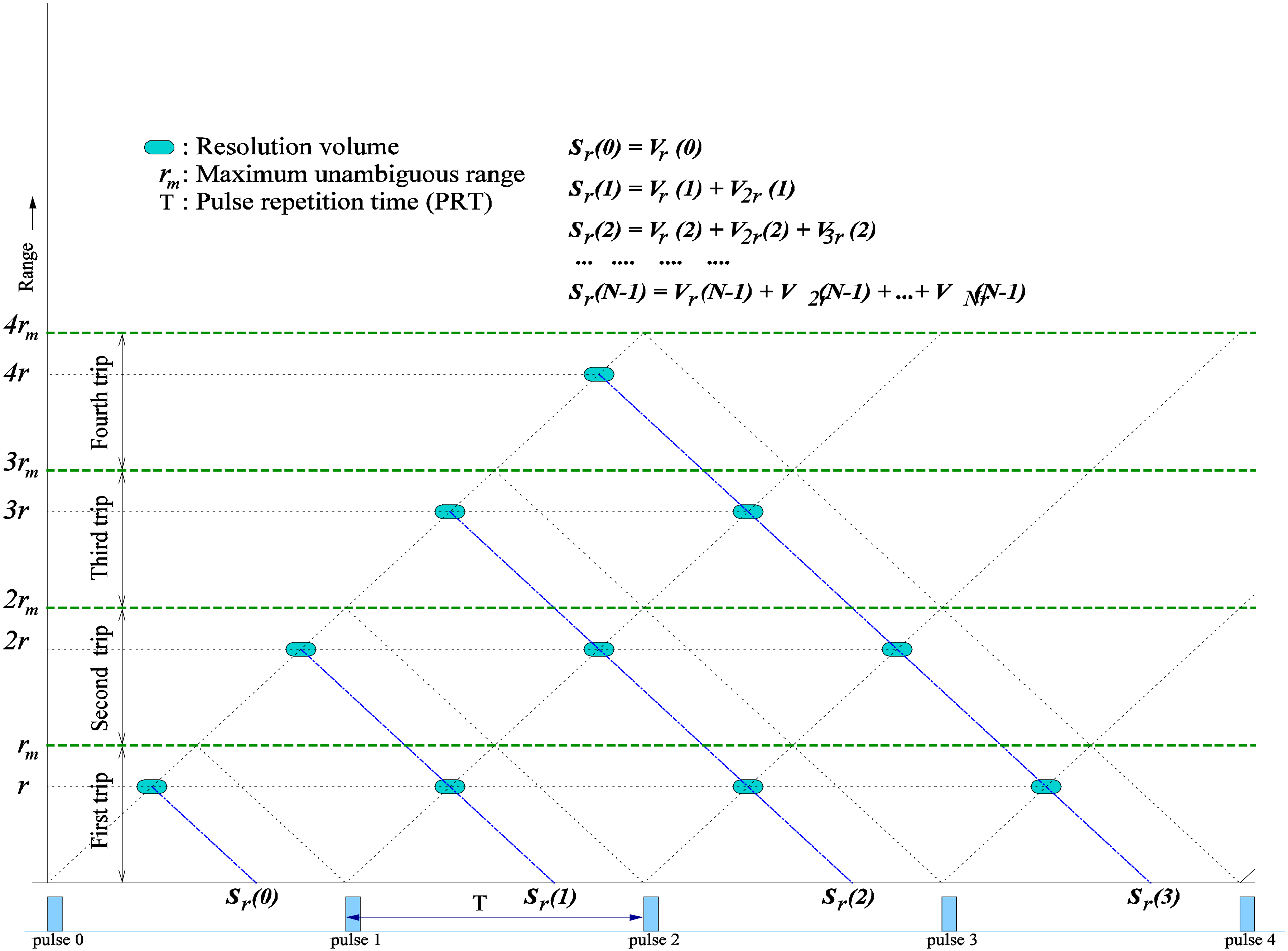

: Resolution volume
r_m : Maximum unambiguous range
T : Pulse repetition time (PRT)
$S_r(0) = V_r(0)$
$S_r(1) = V_r(1) + V_{2r}(1)$
$S_r(2) = V_r(2) + V_{2r}(2) + V_{3r}(2)$
... .
$S_r(N-1) = V_r(N-1) + V_{2r}(N-1) + ... + V_{Nr}(N-1)$
Range
$4r_m$
$4r$
$3r_m$
$3r$
$2r_m$
$2r$
r_m
r
Fourth trip
Third trip
Second trip
First trip
$S_r(0)$
T
$S_r(1)$
$S_r(2)$
$S_r(3)$
pulse 0
pulse 1
pulse 2
pulse 3
pulse 4

The transmitted pulses are phase coded and the received signal is cohered for the first and second trip

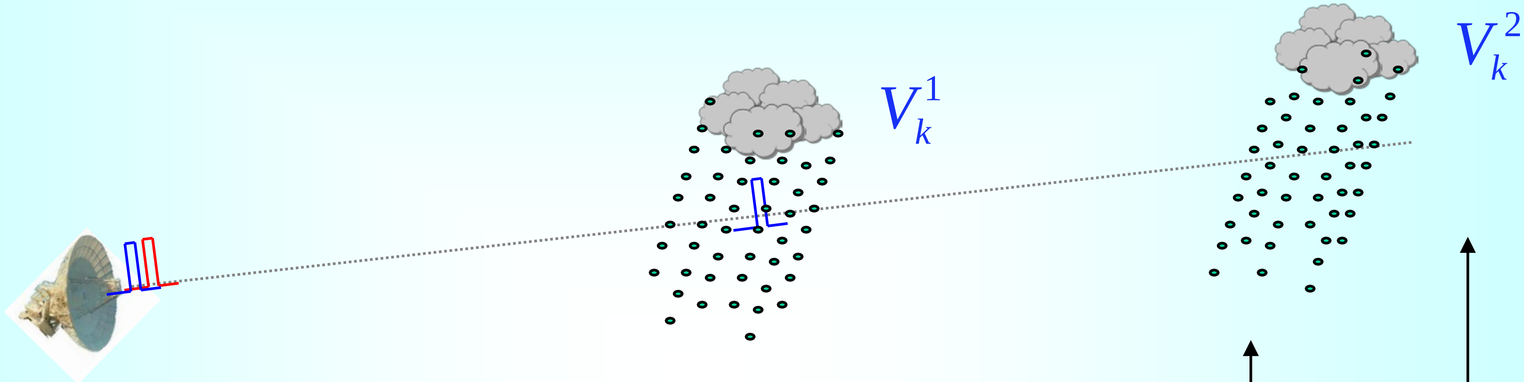

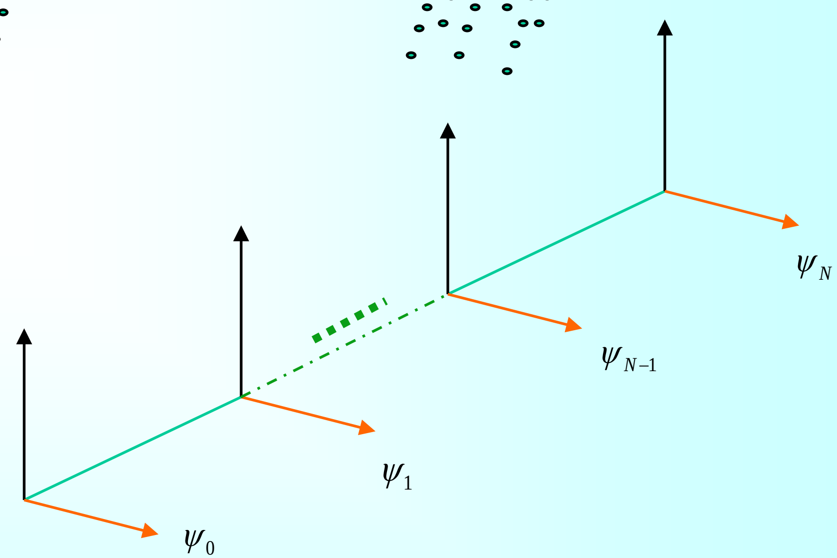

- **The transmitted pulses are phase coded with switching phase ψ_k**

$$V_k = V_k^1 e^{j\psi_k} + V_k^2 e^{j\psi_{k-1}}$$

$$V_k = V_k^1 + V_k^2 e^{j(\psi_{k-1} - \psi_k)}$$

Where $e^{j(\psi_{k-1} - \psi_k)} = e^{j\phi_k}$ **is the modulation code**

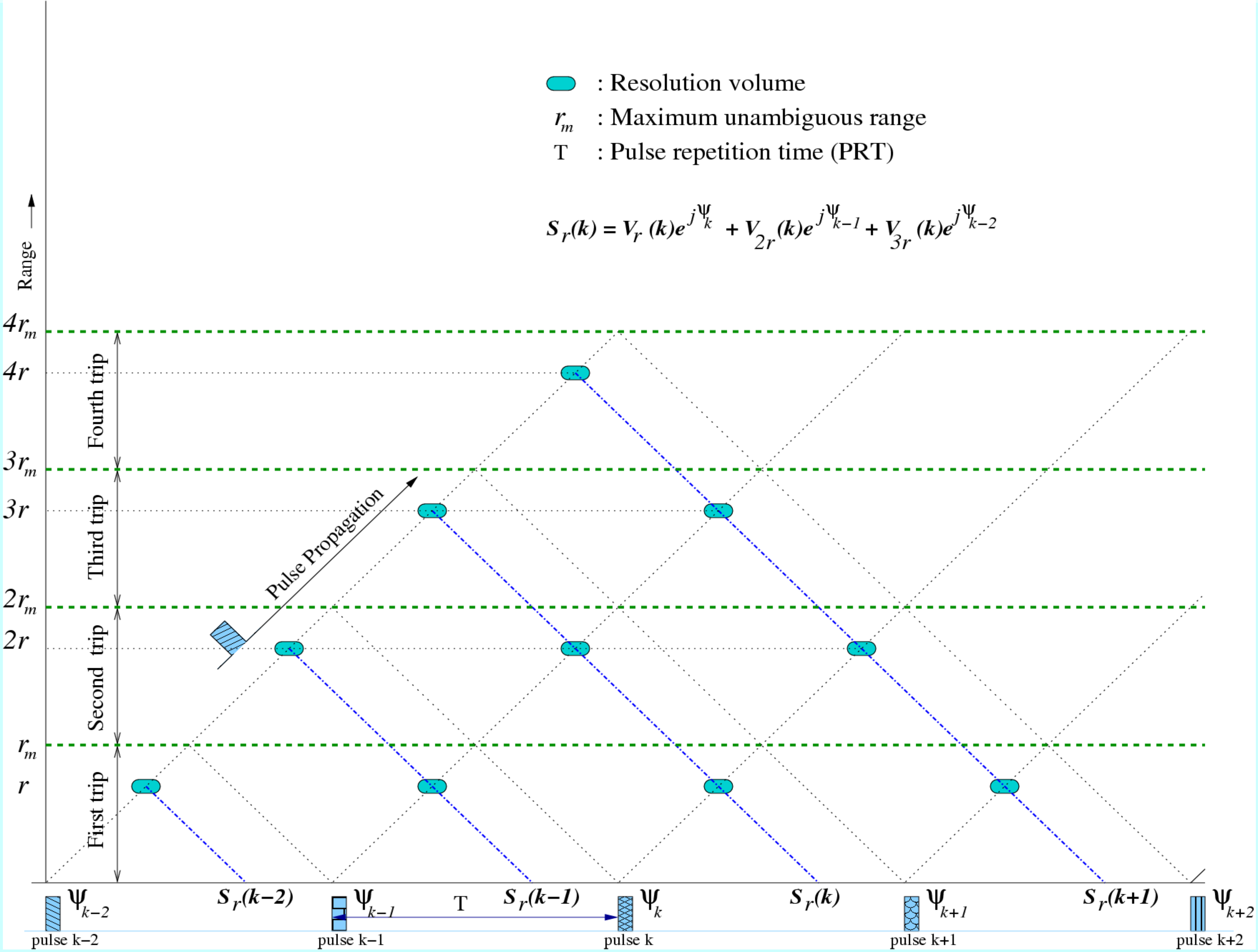

: Resolution volume
r_m : Maximum unambiguous range
T : Pulse repetition time (PRT)
$S_r(k) = V_r(k)e^{j\Psi_k} + V_{2r}(k)e^{j\Psi_{k-1}} + V_{3r}(k)e^{j\Psi_{k-2}}$
Range
$4r_m$
$4r$
$3r_m$
$3r$
$2r_m$
$2r$
r_m
r
Fourth trip
Third trip
Second trip
First trip
Pulse Propagation
Ψ_{k-2}
$S_r(k-2)$
Ψ_{k-1}
T
$S_r(k-1)$
Ψ_k
$S_r(k)$
Ψ_{k+1}
$S_r(k+1)$
Ψ_{k+2}
pulse k−2
pulse k−1
pulse k
pulse k+1
pulse k+2

Random Phase Coding For Range-Overlay Suppression

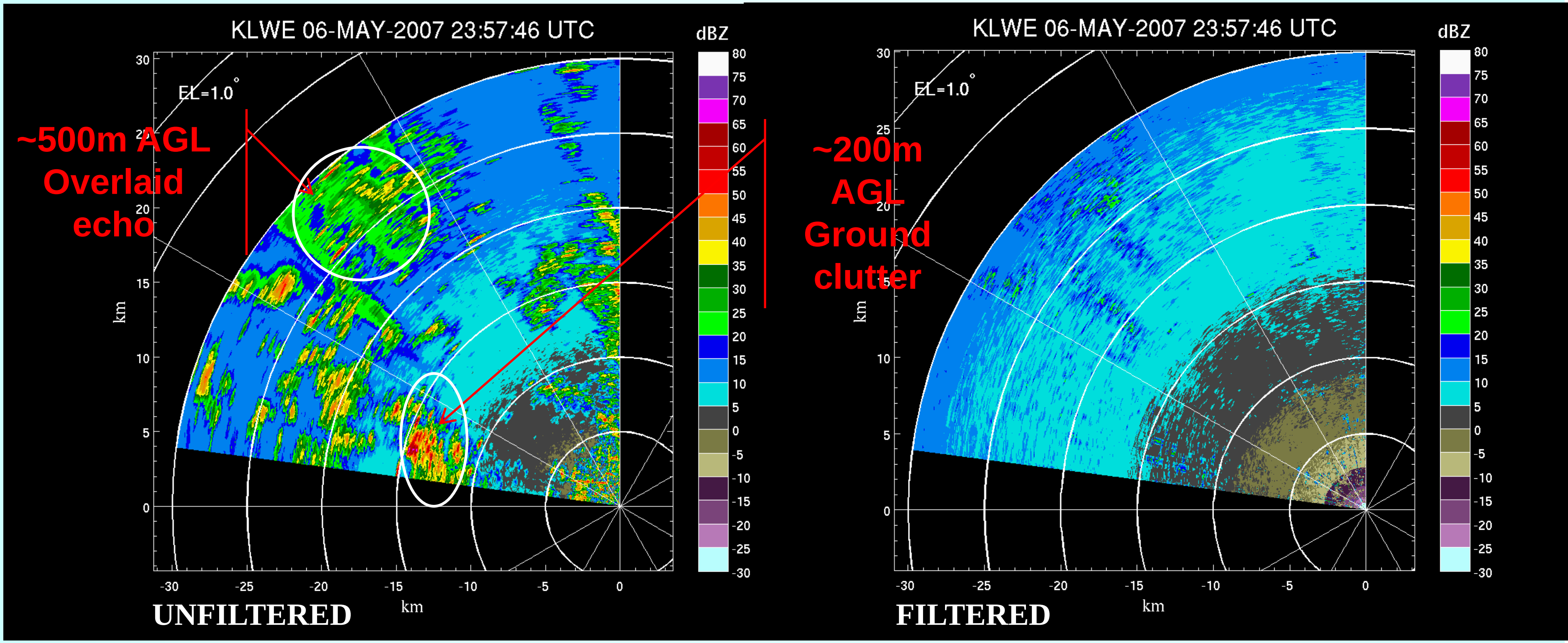

Before overlaid echo suppression and clutter filtering. Data collected on May 06, 2007 at Lawton (EL=1 deg).

After overlaid echo suppression and clutter filtering. Data collected on May 06, 2007 at Lawton (EL=1 deg).

Staggered PRT for Mitigating Velocity Ambiguity

- A periodic block pulsing scheme can be used for range –velocity ambiguity mitigation
- In general we can have $T_1, T_2, T_3, \ldots, T_n$ such that we satisfy

$$\sum_{j=1}^{n} T_j = T$$

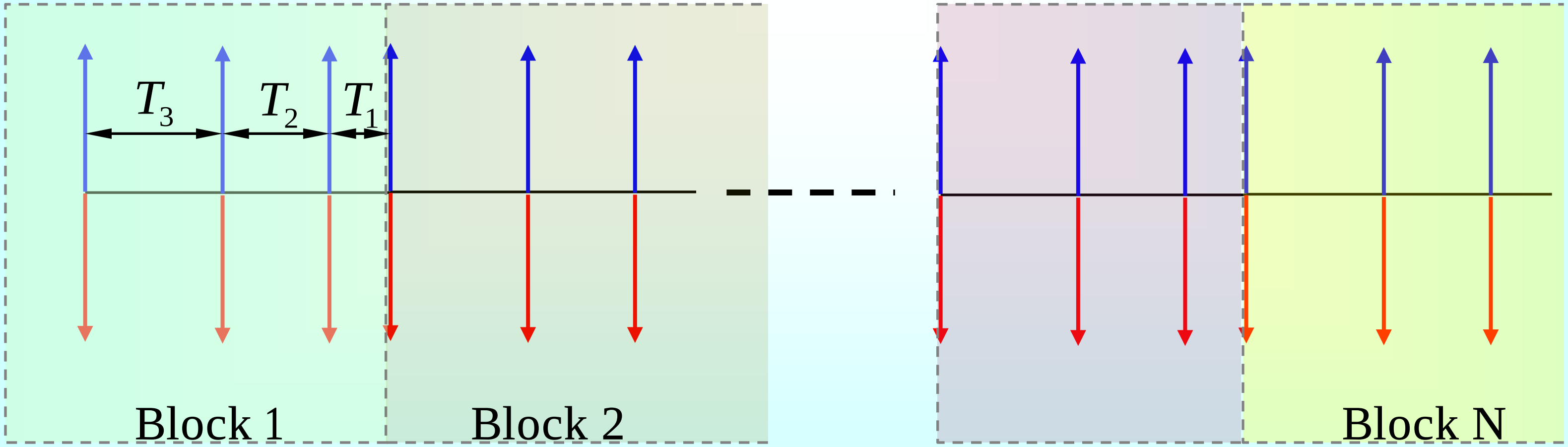

Illustration a periodic block pulsing scheme in hybrid mode of operation for a dual polarized radar

Staggered PRT for Mitigating Velocity Ambiguity

- Staggered PRT scheme with two PRTs T_1 and T_2 will increase the maximum unambiguous velocity to

$$v_a = \frac{\lambda}{4\pi(T_2 - T_1)}$$

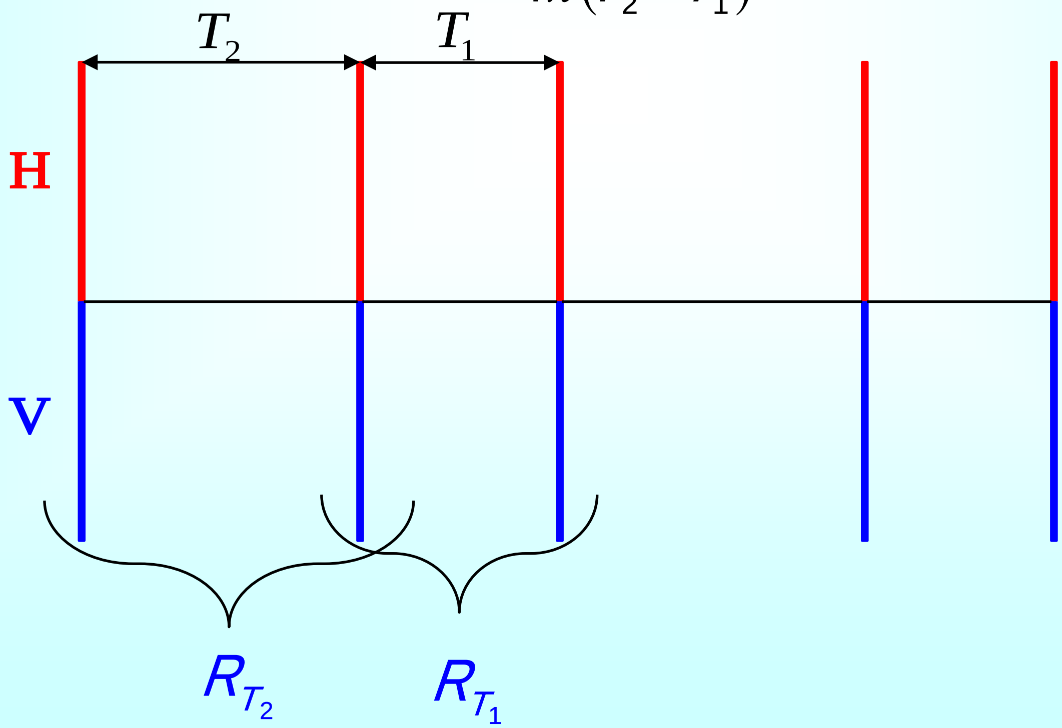

Staggered PRF

- In the staggered PRF technique pulses are transmitted with different PRFs

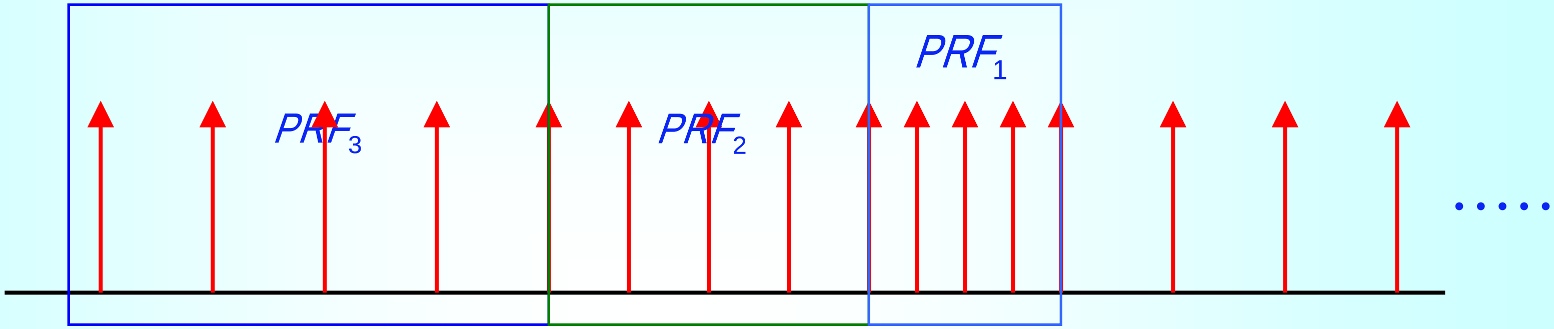

- Dual-PRF waveform are more common in weather radars to increase the unambiguous velocity
- The maximum unambiguous velocity obtained from Dual-PRF waveforms is given by

$$V_a = \frac{V_{a1} V_{a2}}{V_{a1} - V_{a2}}$$

- The unfolding procedure of velocity V_1 is similar to the unfolding procedure of staggered PRT

Velocity Unfolding

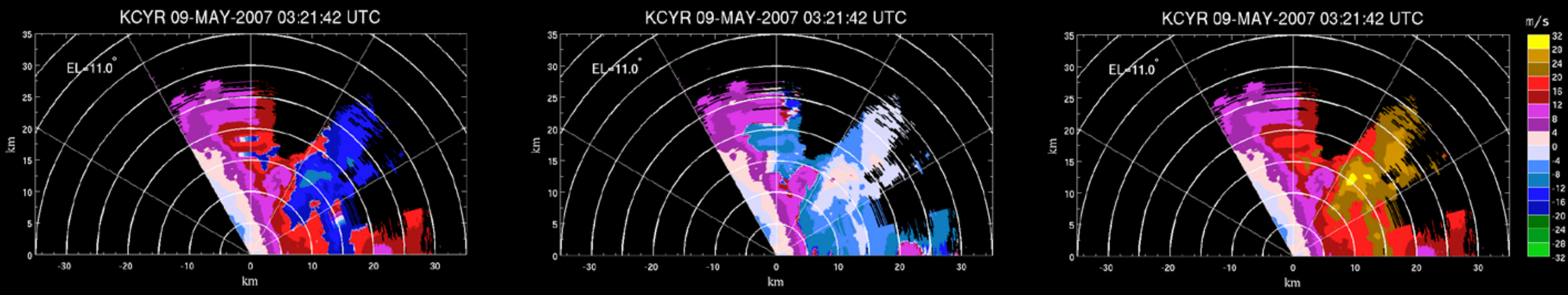

PRF=2.4 kHz **PRF=1.6 kHz** **Unfolded**

Velocity measurements on a radial-by-radial basis with dual-PRF

Unfolded velocity with dual-PRF

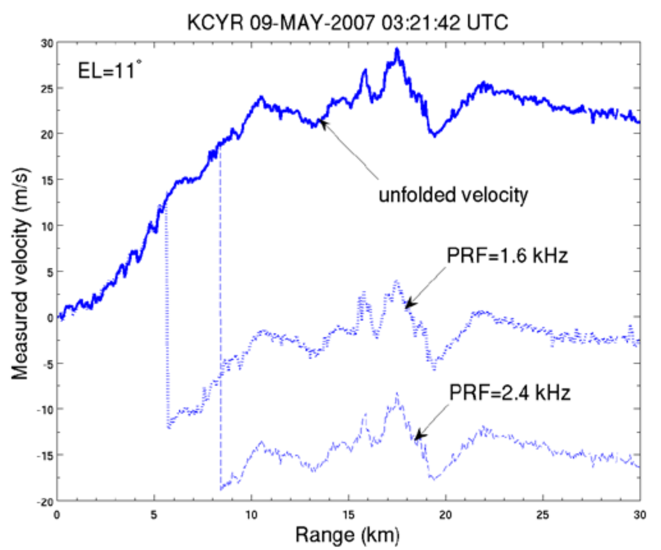

Doppler velocity from Dual-PRF. Data collected on May 09, 2007 at Cyril (EL=11 deg).

Radar Product Generation

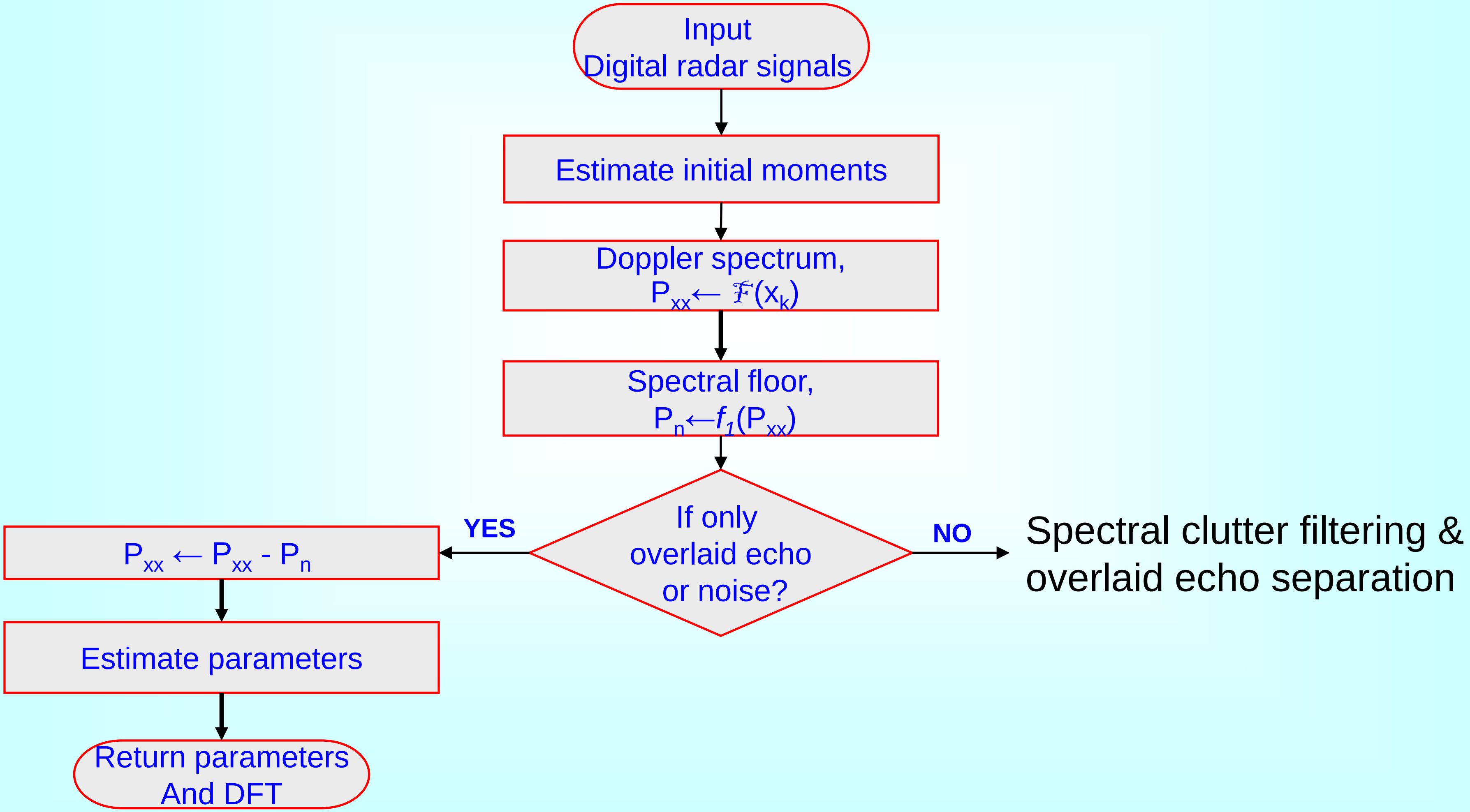

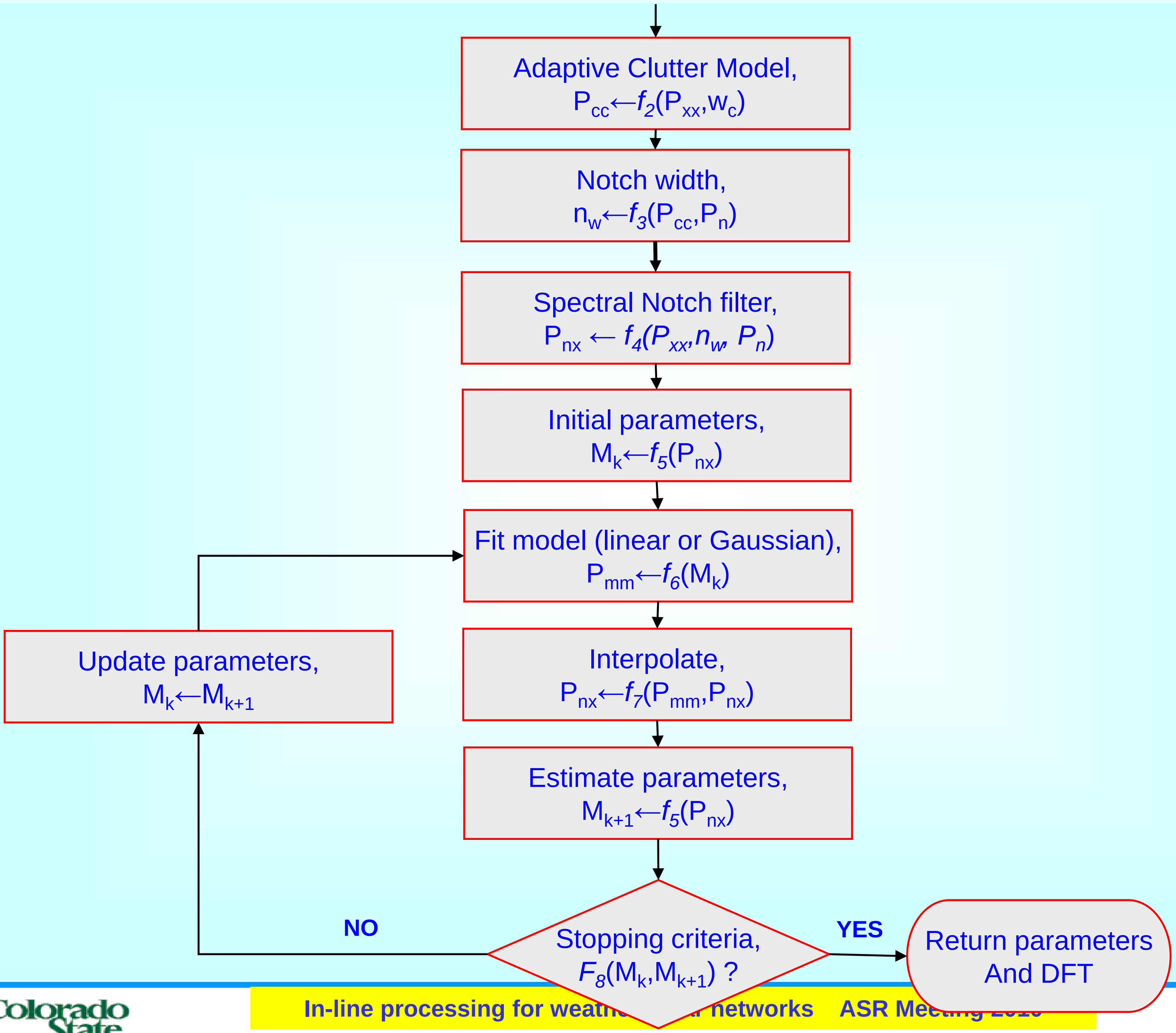
Adaptive Clutter Model,
$P_{cc} \leftarrow f_2(P_{xx}, w_c)$
Notch width,
$n_w \leftarrow f_3(P_{cc}, P_n)$
Spectral Notch filter,
$P_{nx} \leftarrow f_4(P_{xx}, n_w, P_n)$
Initial parameters,
$M_k \leftarrow f_5(P_{nx})$
Fit model (linear or Gaussian),
$P_{mm} \leftarrow f_6(M_k)$
Interpolate,
$P_{nx} \leftarrow f_7(P_{mm}, P_{nx})$
Estimate parameters,
$M_{k+1} \leftarrow f_5(P_{nx})$
Update parameters,
$M_k \leftarrow M_{k+1}$
Stopping criteria,
$F_8(M_k, M_{k+1})$?
NO
YES
Return parameters
And DFT

- f_1= Dynamic noise floor estimation
- f_2= Adaptive clutter model
- f_3= Adaptive notch width
- f_4= Spectral notch filter
- f_5= Moments estimation from spectrum
- f_6= Spectral model
- f_7= Interpolation
- f_8= Iteration stopping criteria
- f_9= Calibrated Zh calculation
- f_{10}= Calibrated Zdr calculation
- f_{11}= Differential propogation phase
- f_{12}= Co-polar correlation coefficient
- f_{13}= Dual-PRF velocity unfolding
- f_{14}= Speckle filter

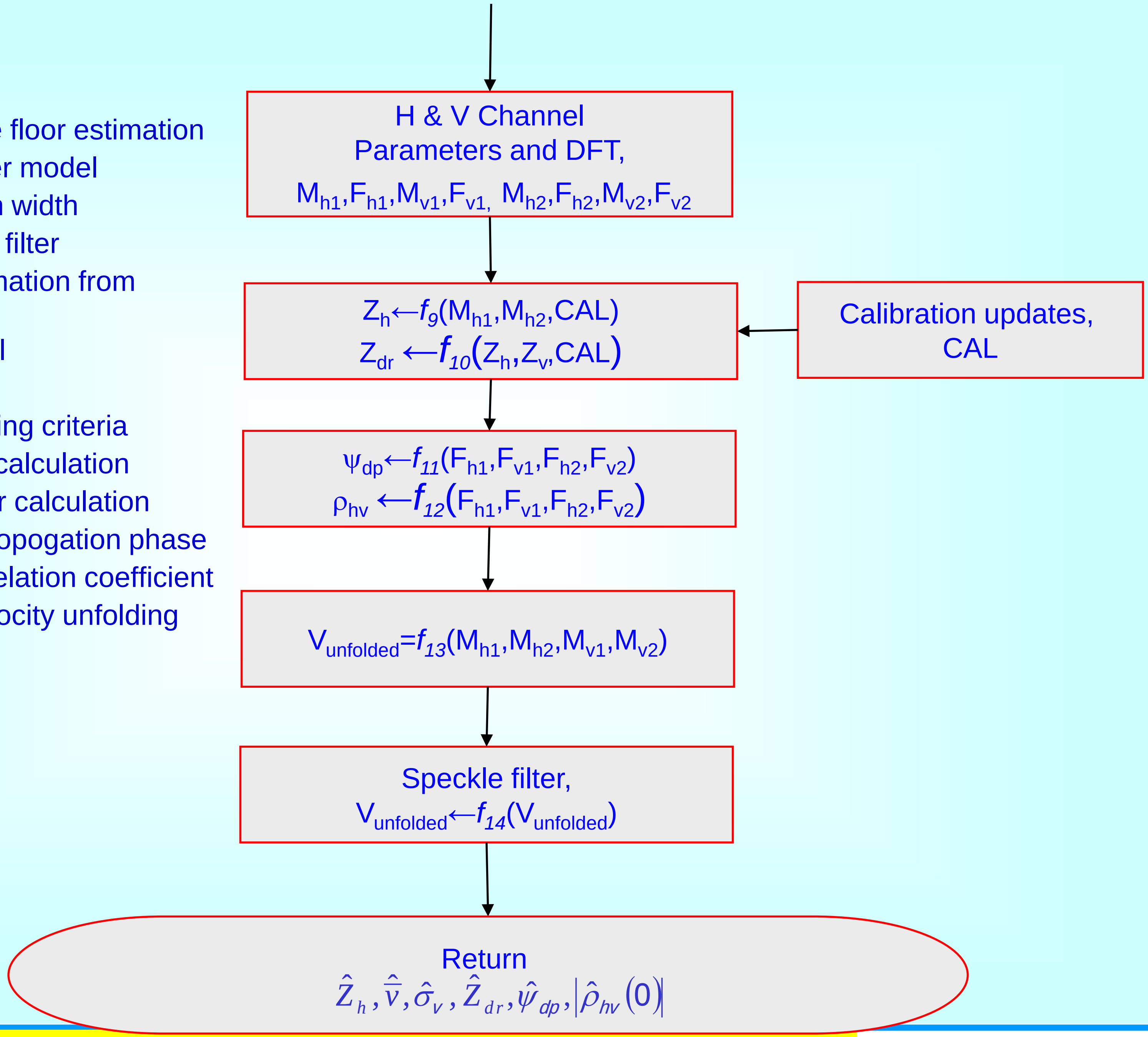

Data Products with CSU-CHILL

Data collected with PRT =1 ms; N=64 on Dec 20, 2006 at 23:58:19 UTC

Severe clutter from Rocky mountains

Velocities biased due to clutter

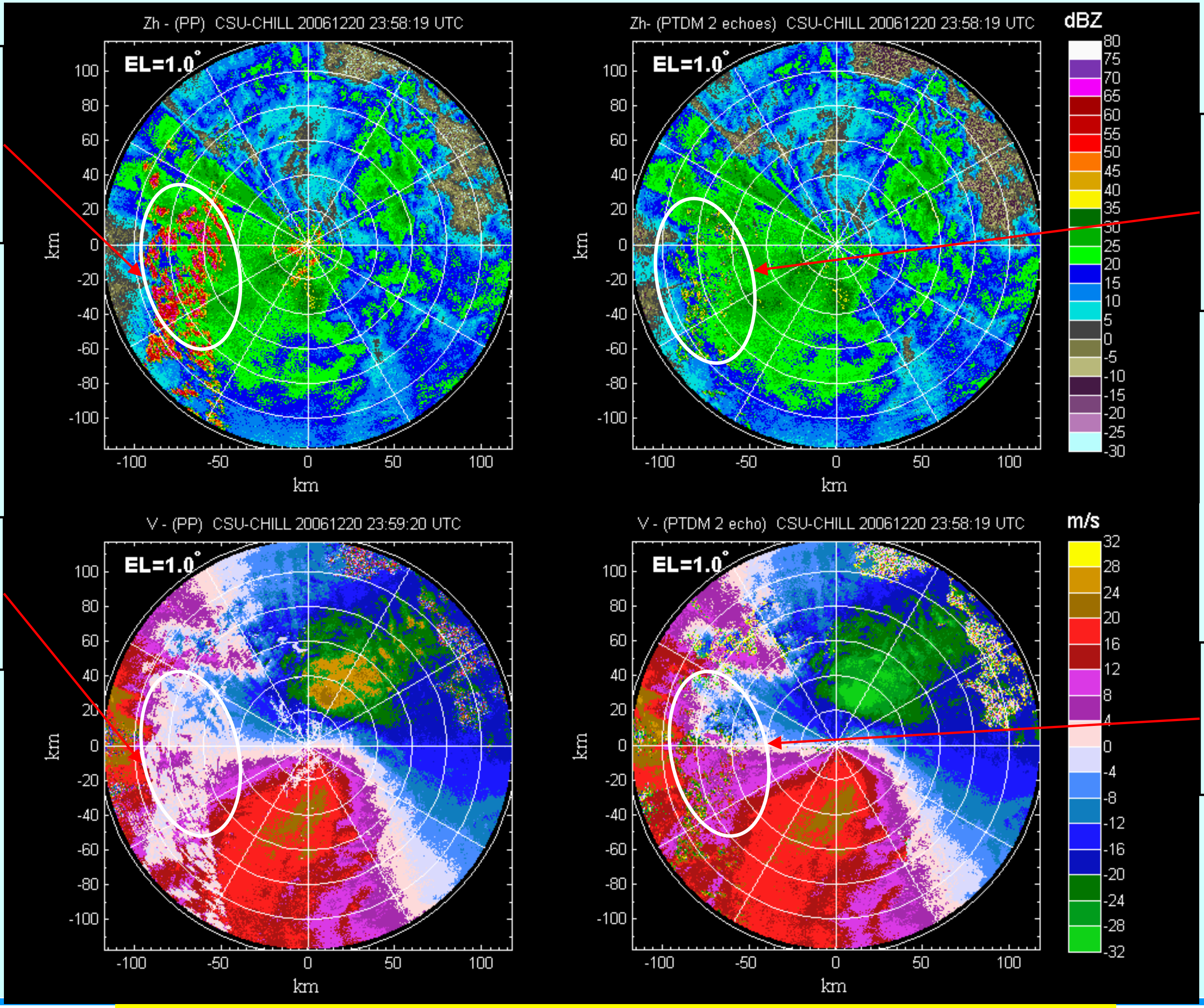

Reflectivity after spectral clutter filtering

Velocities after clutter filtering

Attenuation correction

IP1 Real-time Dual-Pol Based Attenuation Correction

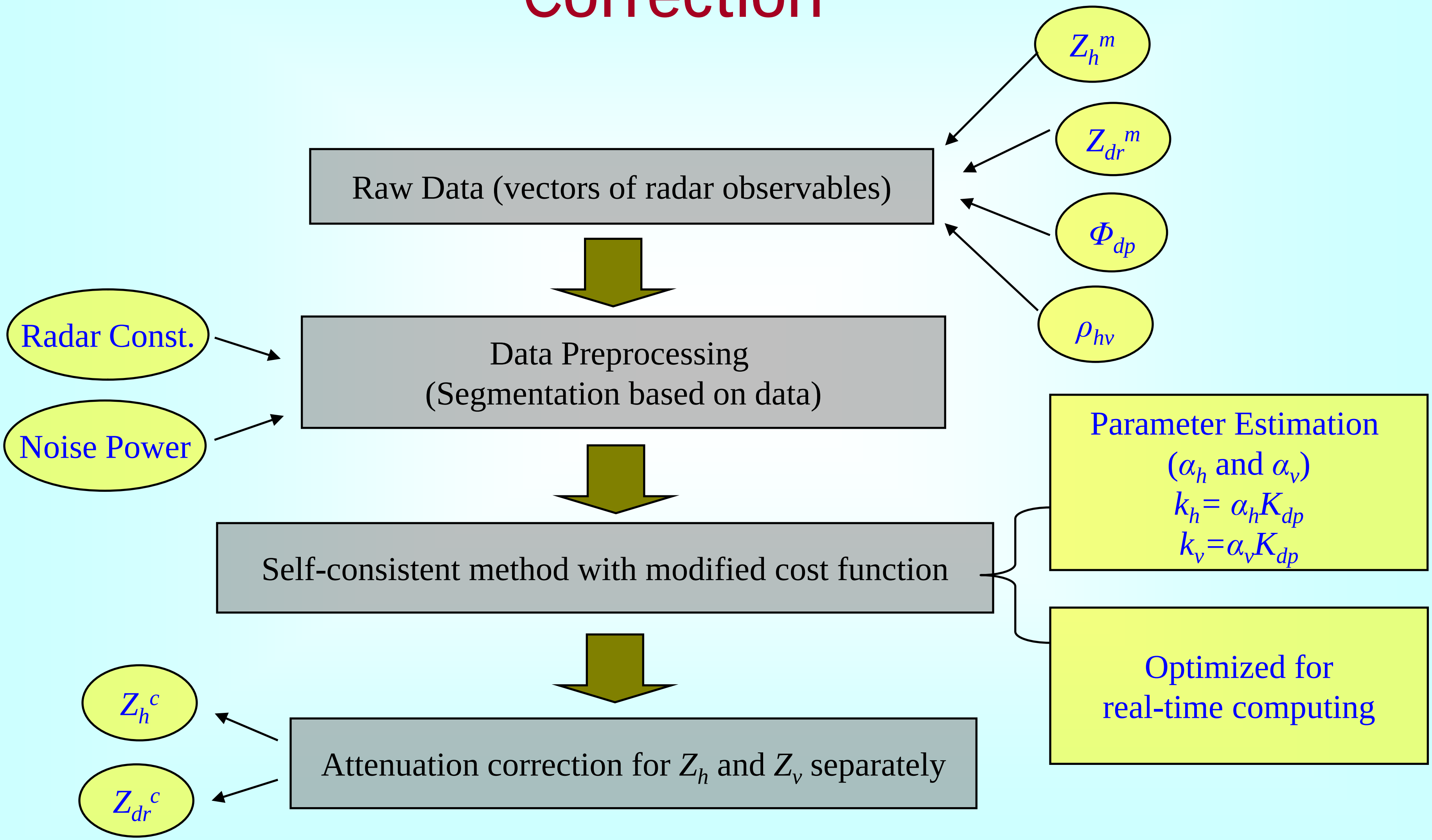

Dual-Pol Based Attenuation Correction

Reflectivity maps at 07:37:31 May 8 2007 and Nexrad reflectivity map at 07:37:24 May 8 2007. (a) IP1 reflectivity before attenuation correction (b) IP1 reflectivity after attenuation correction (c) Nexrad reflectivity.

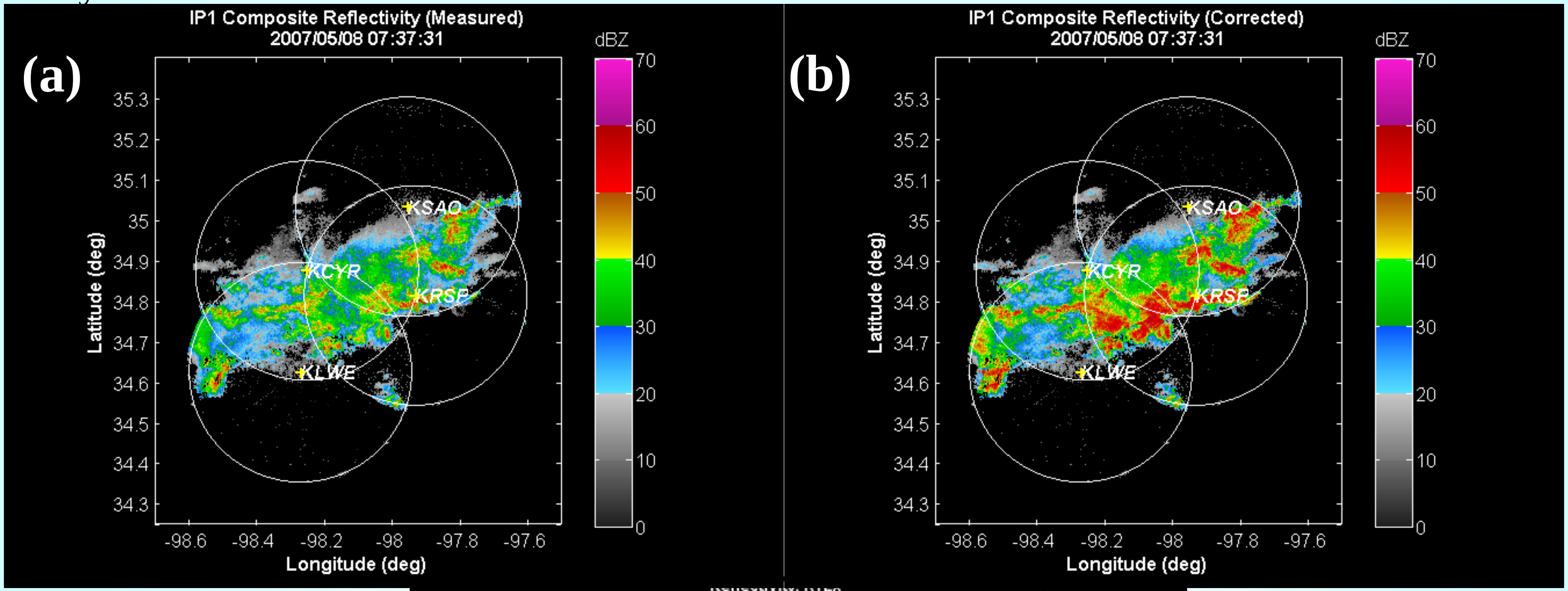

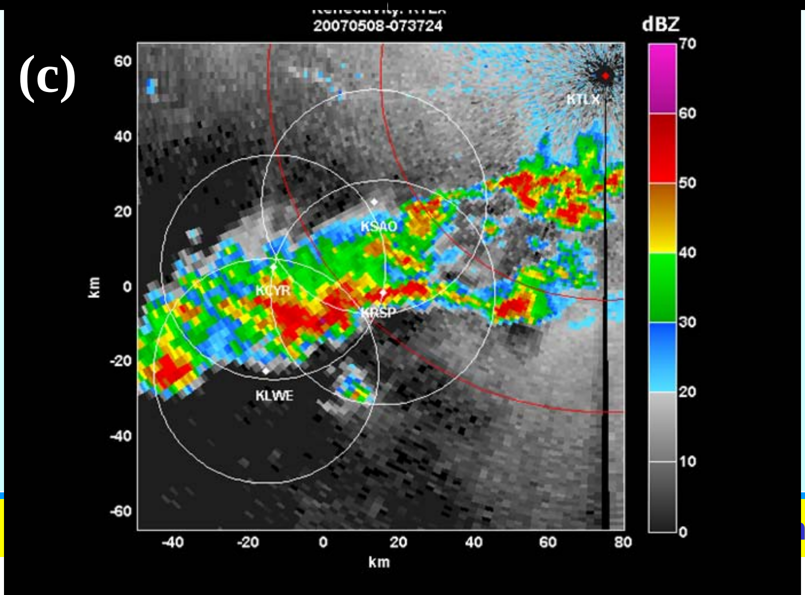

Dual-Pol Based Attenuation Correction

Z_{dr}-Z_h and K_{dp}-Z_h 2D histogram plots for a squall line case on May 8, 2006 before and after attenuation correction.

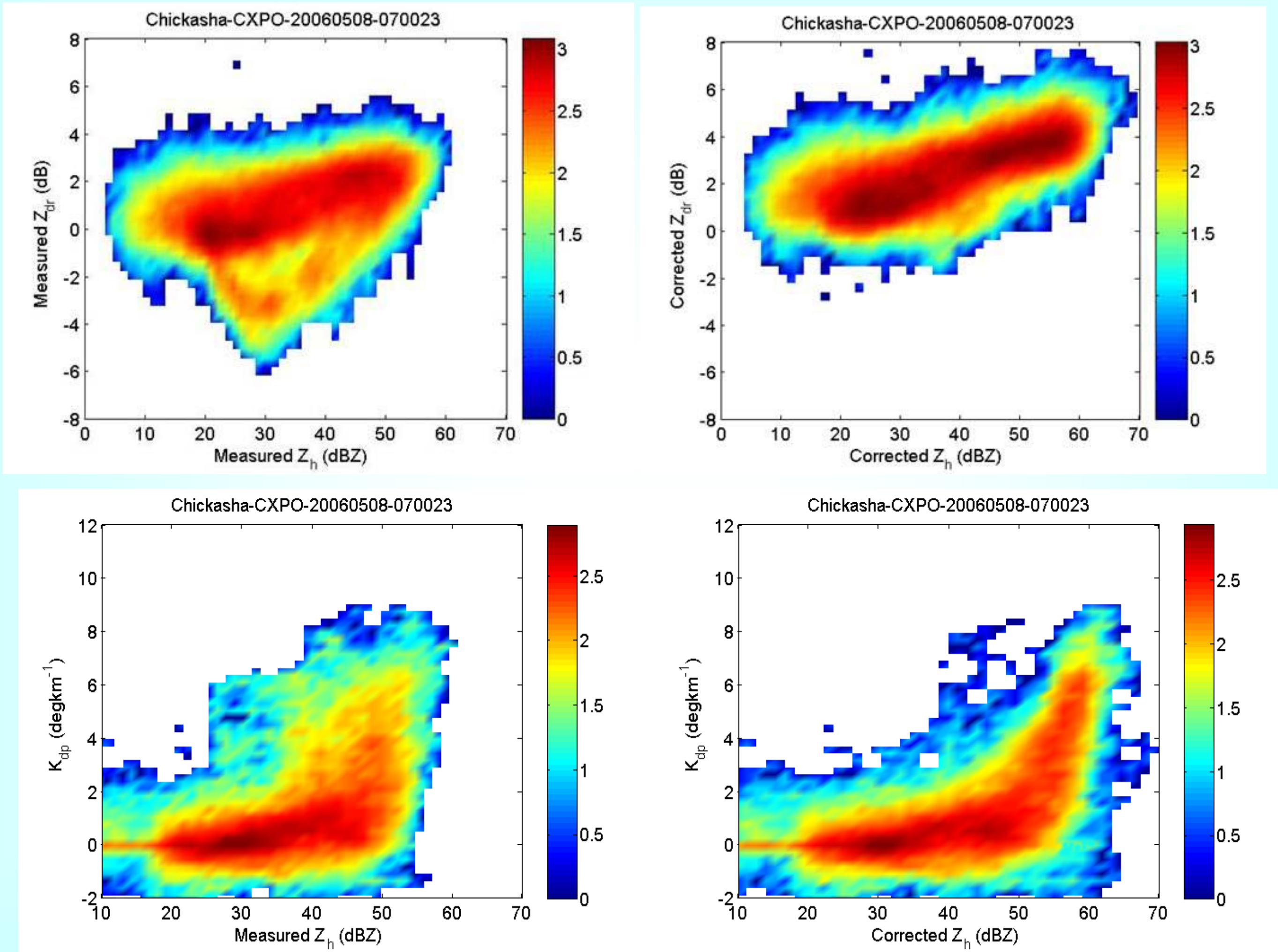

Z_{dr}-Z_h

K_{dp}-Z_h

Before attenuation correction

After attenuation correction

QPE

Rainfall Algorithms

$$R(Z, Z_{dr}) = CZ_h^a \mathcal{Z}_{dr}^b \quad \text{or} \quad CZ_h^a 10^{0.1bZ_{dr}(dB)}$$

$$R(K_{dp}) = 129\left(\frac{K_{dp}}{f}\right)^{b_2}$$

$$R(K_{dp}, Z_{dr}) = C_3 K_{dp}^{a_3} \mathcal{Z}_{dr}^{b_3} \qquad \text{mm h}^{-1}$$

The use of K_{dp} to estimate rainfall has a number of advantages over power measurements:

- independent of receiver and transmitter calibrations,
- unaffected by attenuation,
- relatively immune to beam blockage,
- unbiased by presence of hail or other 'spherical' ice particles in the resolution volume

- The radar network
  - Southwestern Oklahoma, ~7000 sq km
  - Four X-band, dual-polarization radar

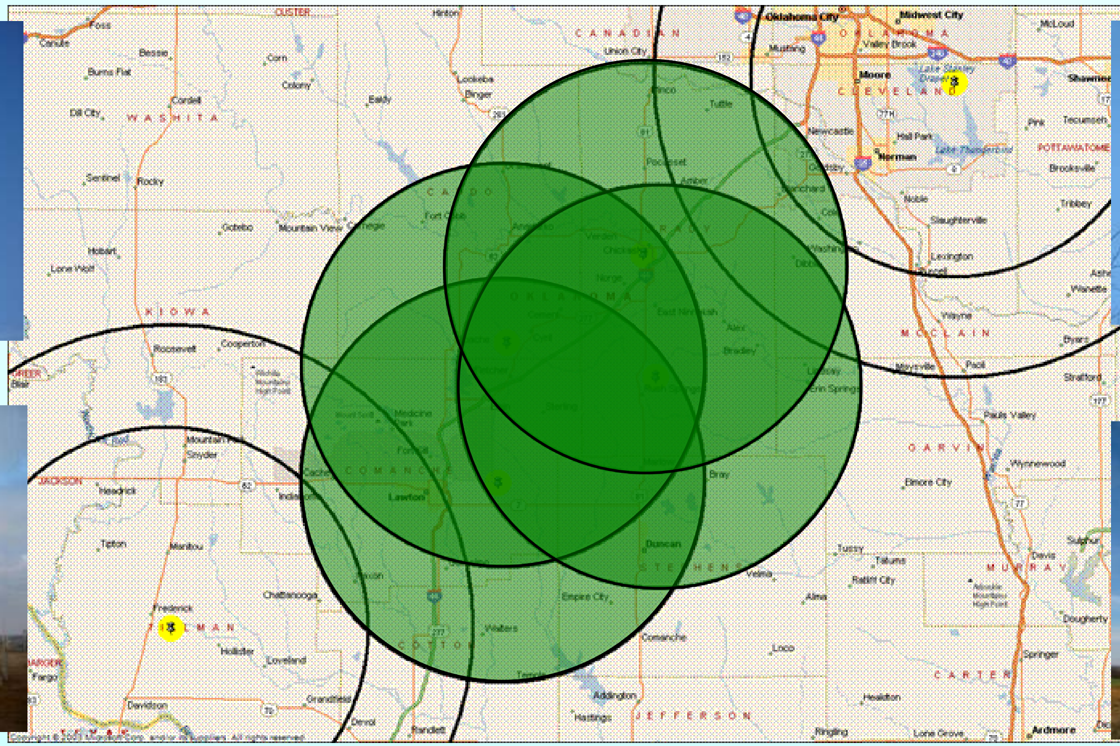

NIED's X-Net Test Bed

- Led by NIED, National Research Institute for Earth Science and Disaster Prevention, Japan
  - Over one of the most populous and densest metropolitan regions in the world

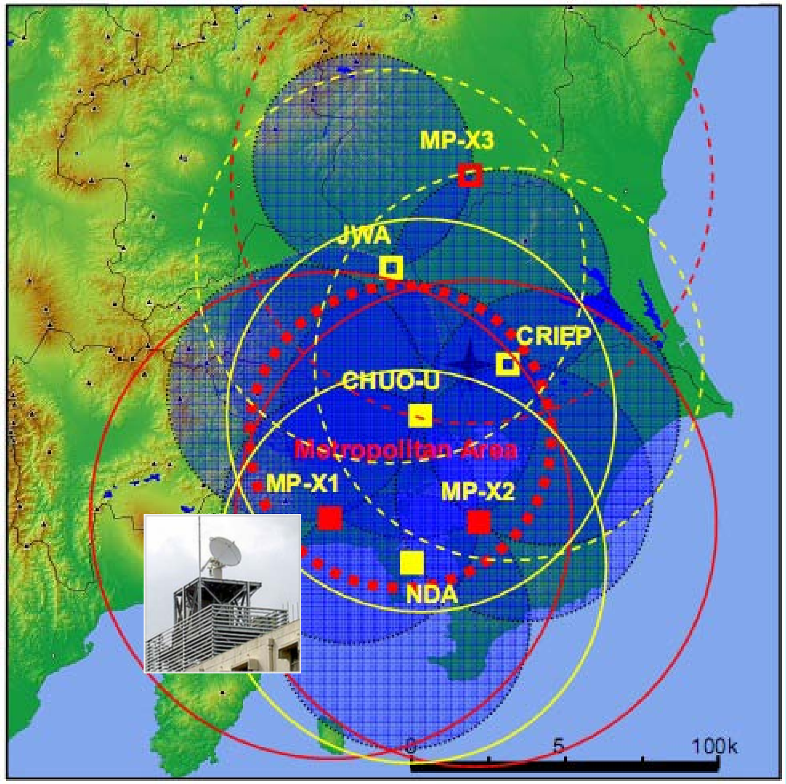

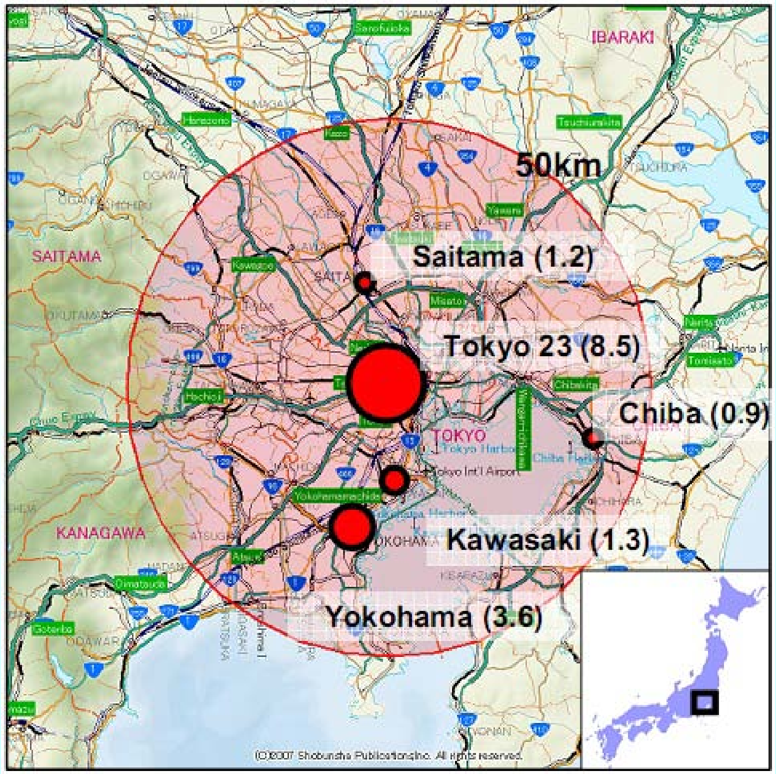

K_{dp} and Composition

- K_{dp} based rainfall conversion is attractive at X-band
  - Responds well to low rainfall rate
  - Avoids the uncertainty in attenuation correction
  - Immune to calibration factors across the network

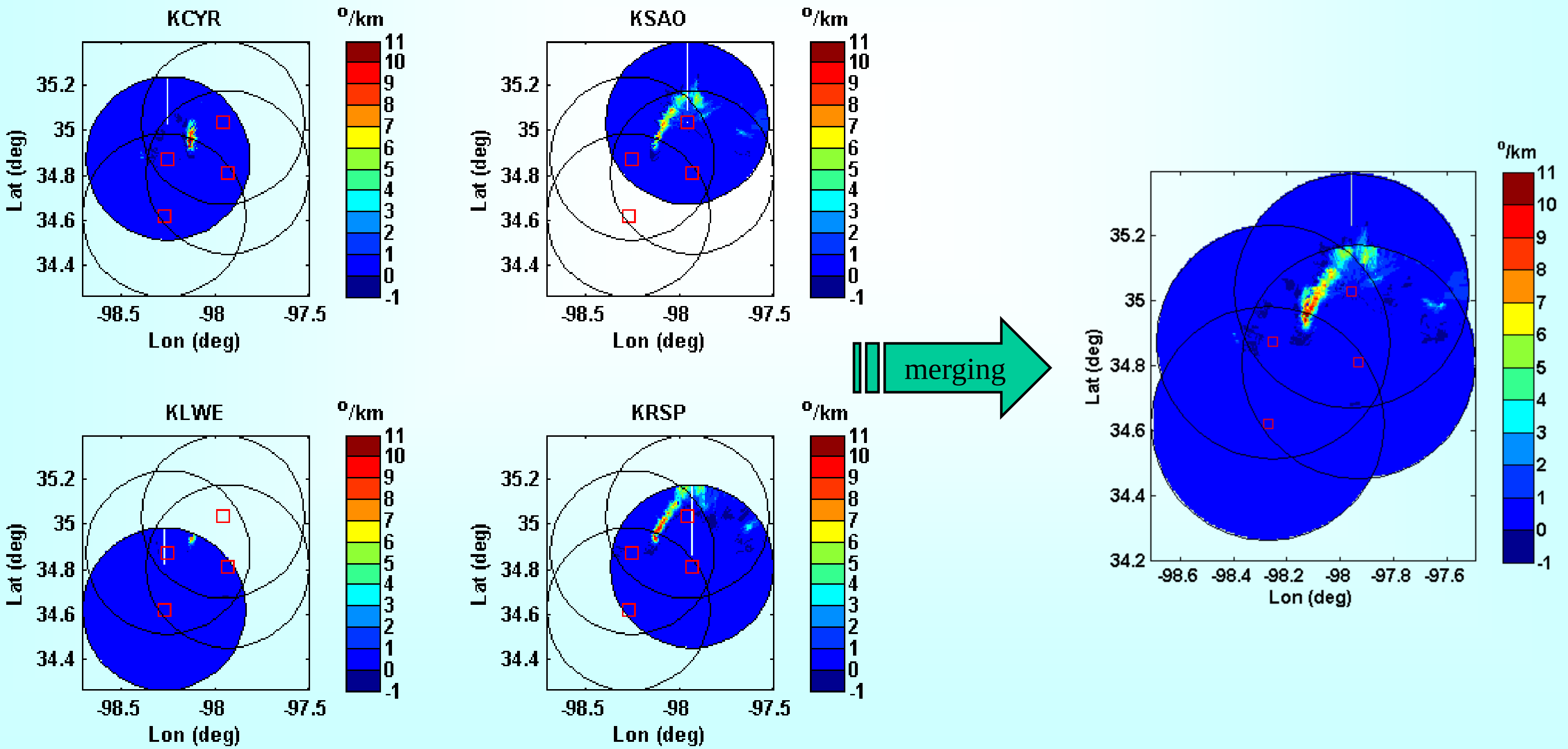

Rainfall Conversion

- *R-K*$_{dp}$ based rainfall estimation was implemented in CASA's IP1 test bed.

$$R = 0.6\pi \times 10^{-3} \int v(D) D^3 N(D) dD$$

$$K_{dp} = \frac{\pi^2}{6\lambda} C \int (1-r) D^3 N(D) dD$$

A scaled version of KOUN's rainfall estimation is tested (based on local measured DSDs). *

$$R = 47.3 K_{dp}^{0.791} \text{ mm/hr}$$

⇓

$$R = 18.15 K_{dp}^{0.791} \text{ mm/hr}$$

***** Ryzhkov, A.V., S.E. Giangrande, and T.J. Schuur, 2005: Rainfall Estimation with a Polarimetric Prototype of WSR-88D. J. Appl. Meteor., **44**, 502–515.

Gauge Comparison

- USDA ARS Micronet – A rain gauge network located at the center of the IP1 test bed

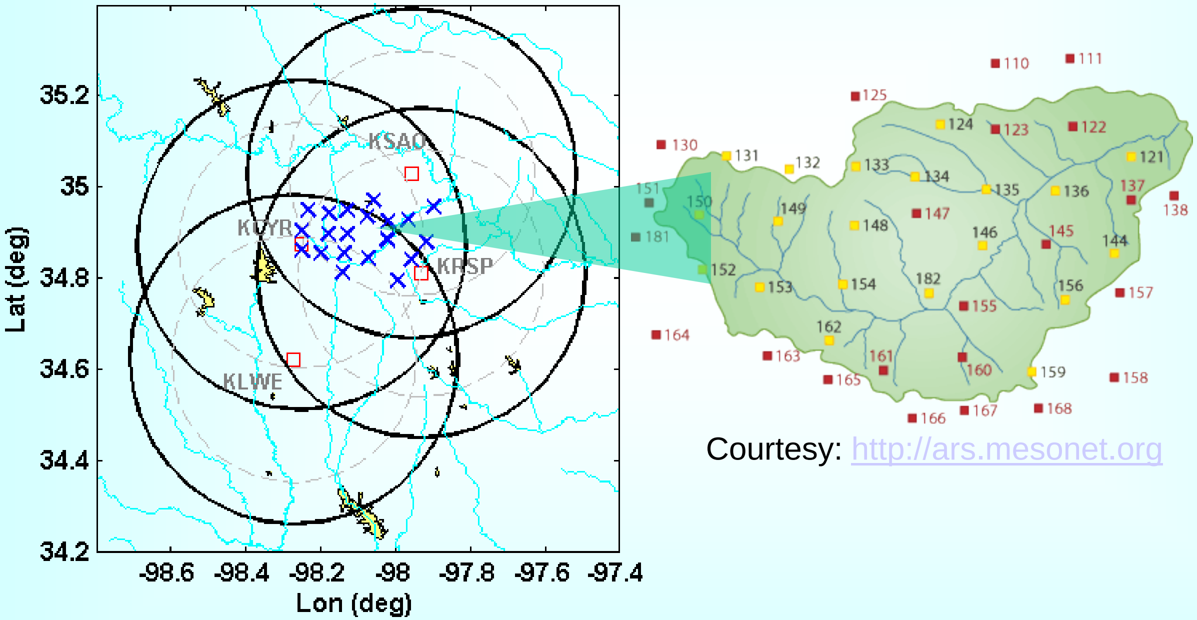

Courtesy: http://ars.mesonet.org

Little Washita

Size: 611 km^2

Mean annual precipitation: 760 mm

Gauge network: 20 tip-bucket stations

QPE Evaluation

- Metrics:
  - Normalized bias: $$< e >_N = \frac{\langle R_R - R_G \rangle}{\langle R_G \rangle}$$
  - Normalized error: $$NSE = \frac{\langle |R_R - R_G| \rangle}{\langle R_G \rangle}$$

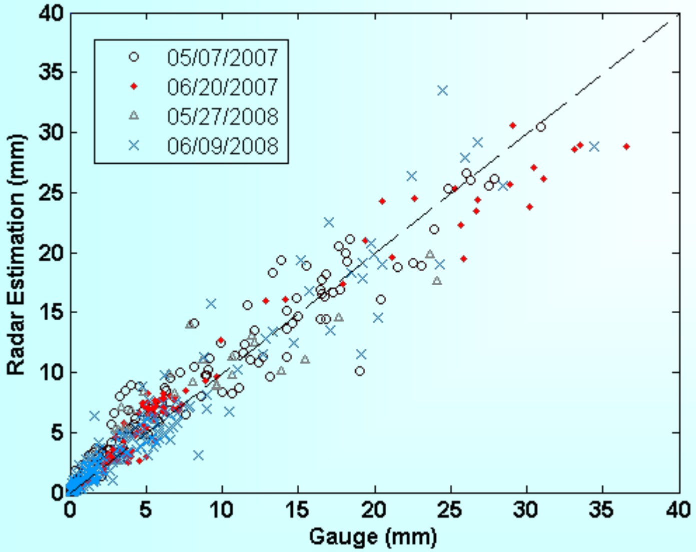

Performance of hourly rainfall estimates in comparable weather radar systems using K_{dp} based QPE algorithms.

Radar System or Network	Total Events Analyzed	NSE (%)
IP1(total)	29	22.76
Instantaneous		42
Hourly		15
MP-X	3	14.8

QPE Evaluation

- A composite R-K_{dp} based estimation was implemented in NIED's X-Net test bed.
- X-Net Ground Validation
  - Three events: 2 straitform, 1 typhoon

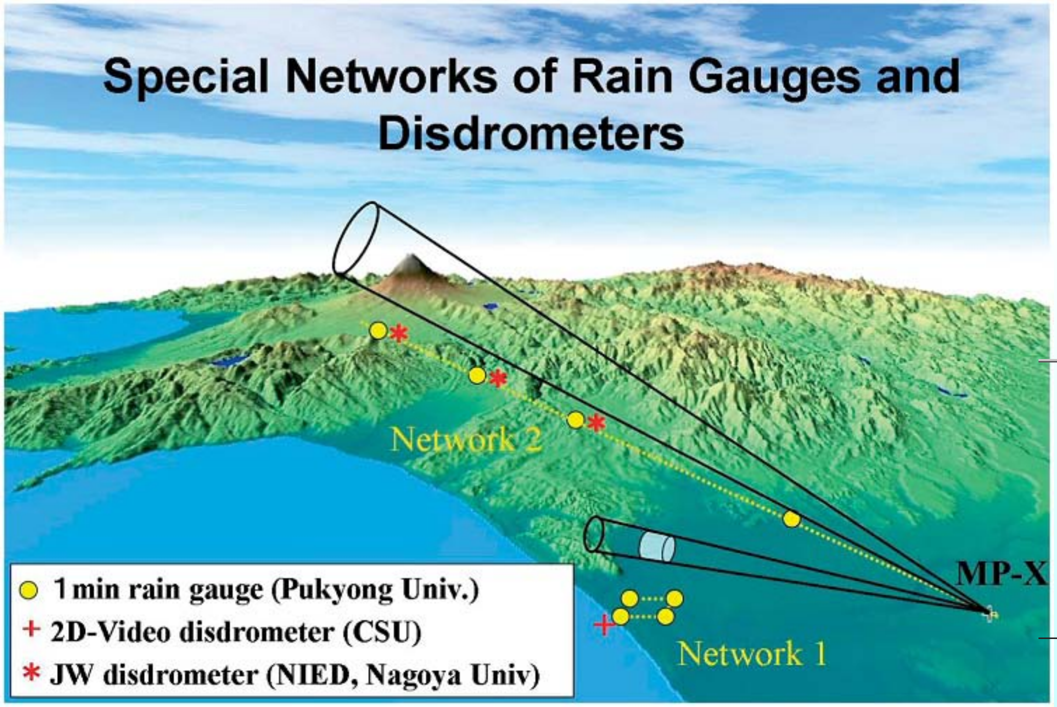

$$R = 19.63 K_{dp}^{0.823} \text{ mm/hr}$$

$$K_{dp} > 0.3^{o}/km \text{ and } Z_h > 35 dBZ$$

$$R = 7.07 \times 10^{-3} Z_h^{0.819} \text{ mm/hr}$$

Also based on locally measured DSDs

15 min	NE (%)	21.1
	NB (%)	−2.9
1 h	NE (%)	14.8
	NB (%)	−1.1
3 h	NE (%)	11.4
	NB (%)	−1.0

Dual Doppler

Dual-Doppler Scan and Retrieval

- Real-time Dual-Doppler wind velocity retrieval system has been developed and installed in IP1, based on proven algorithms and computation tools.
  - 3-D observations from the IP1 radars are gridded and merged, fused into a common analysis grid
  - Both horizontal wind field and vertical wind component are computed

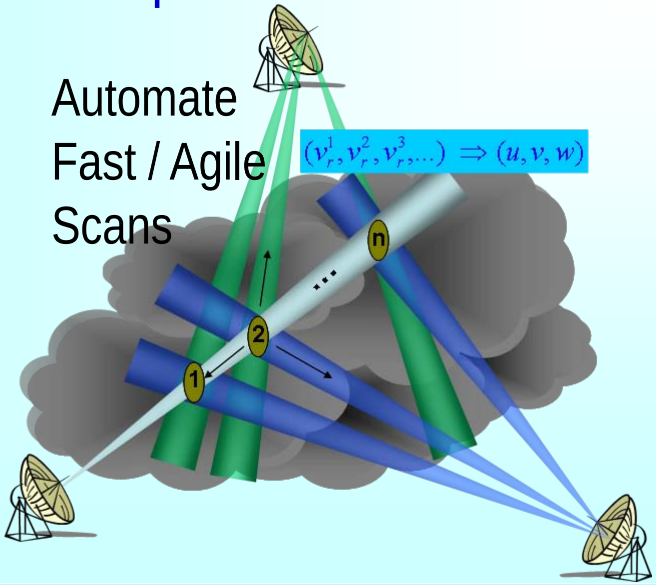

$$\begin{bmatrix} u \\ v \end{bmatrix} = \begin{bmatrix} \sin\phi_1\cos\theta_1 & \cos\phi_1\cos\theta_1 \\ \sin\phi_2\cos\theta_2 & \cos\phi_2\cos\theta_2 \end{bmatrix}^{-1} \begin{bmatrix} v_r^1 \\ v_r^2 \end{bmatrix} + \begin{bmatrix} \sin\phi_1\cos\theta_1 & \cos\phi_1\cos\theta_1 \\ \sin\phi_2\cos\theta_2 & \cos\phi_2\cos\theta_2 \end{bmatrix}^{-1} \begin{bmatrix} \sin\theta_1 \\ \sin\theta_2 \end{bmatrix} (w + w_t)$$

low level approximation

Dual-Doppler Scan and Retrieval

- The upgrades over the last two storm seasons improved the capability of the IP1 radar network for dual-Doppler wind observations

Error assessment at lower altitudes

$$\frac{\sigma_{u'}^2+\sigma_{v'}^2}{2\sigma_{v_r}^2}=\frac{1}{\sin^2(\phi_1-\phi_2)}\frac{\cos^2\theta_1+\cos^2\theta_2}{2\cos^2\theta_1\cos^2\theta_2}$$

Unique Capabilities

- Real-time processing and control

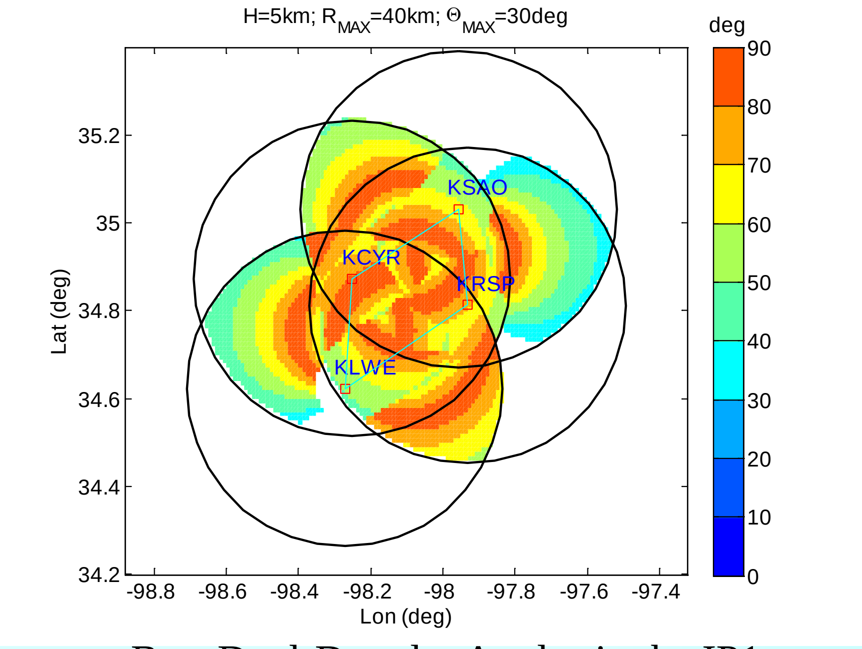

Best Dual-Doppler Angles in the IP1 Coverage at 5 km AGL

Dual-Doppler Scan and Retrieval

- Dual-Doppler scan strategy
  - Best beam crossing angle for Dual-Doppler retrieval;
  - Lowest elevation angle to reduce scan interval (tilts);
  - Closest range to efficiently use the power budget.

$$F = \frac{\sigma_{u'}^2 + \sigma_{v'}^2}{2\sigma_{v_r}^2} + \left(\frac{\max(\theta_1, \theta_2)}{\theta_{MAX}}\right)^2 + \left(\frac{\max(r_1, r_2)}{r_{MAX}}\right)^2$$

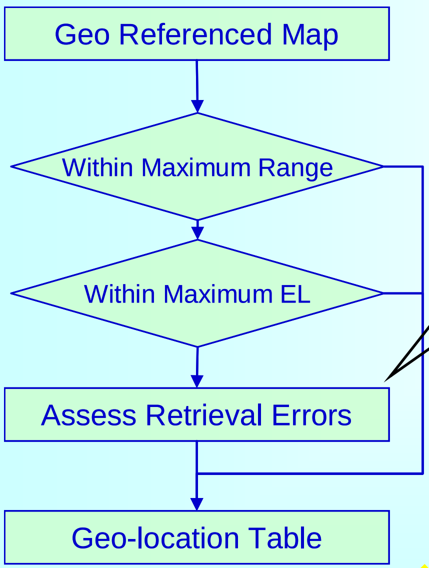

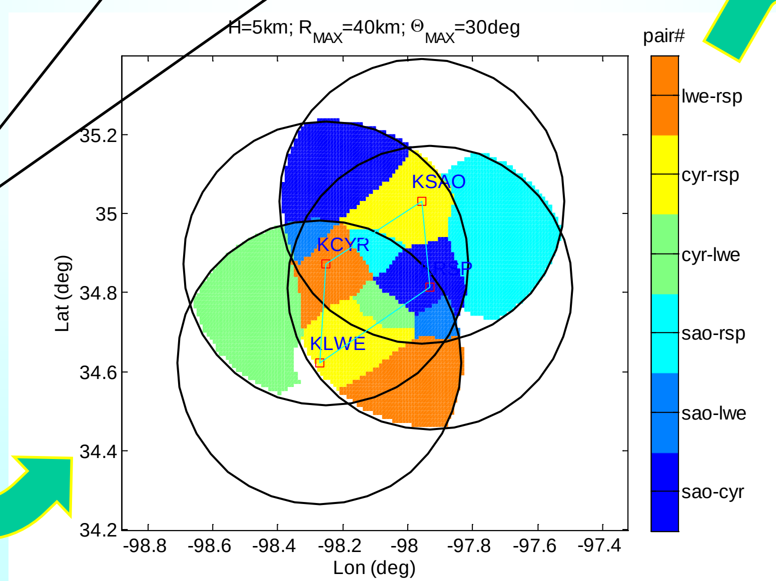

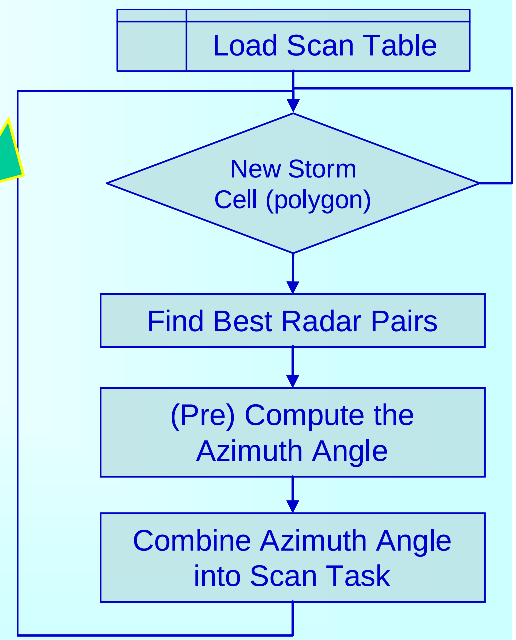

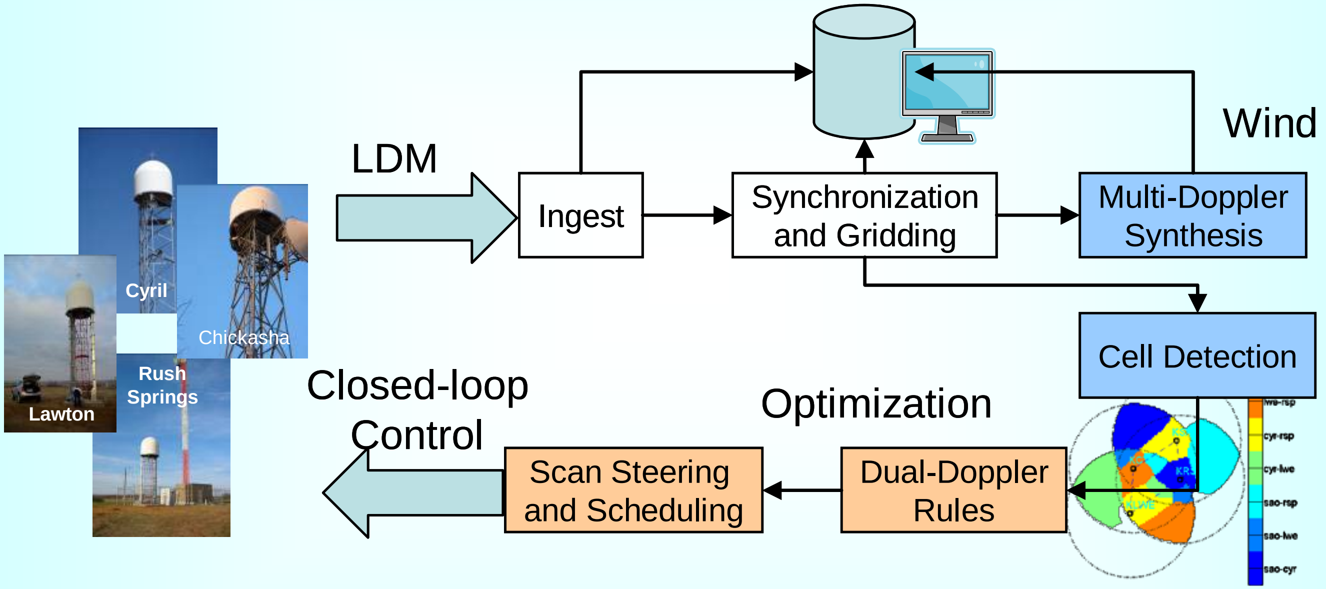

Cyril
Chickasha
Lawton
Rush Springs
LDM
Ingest
Synchronization and Gridding
Multi-Doppler Synthesis
Wind
Cell Detection
Optimization
Dual-Doppler Rules
Scan Steering and Scheduling
Closed-loop Control

Anadarko Tornado and Damaging Winds Event – May 13, 2009

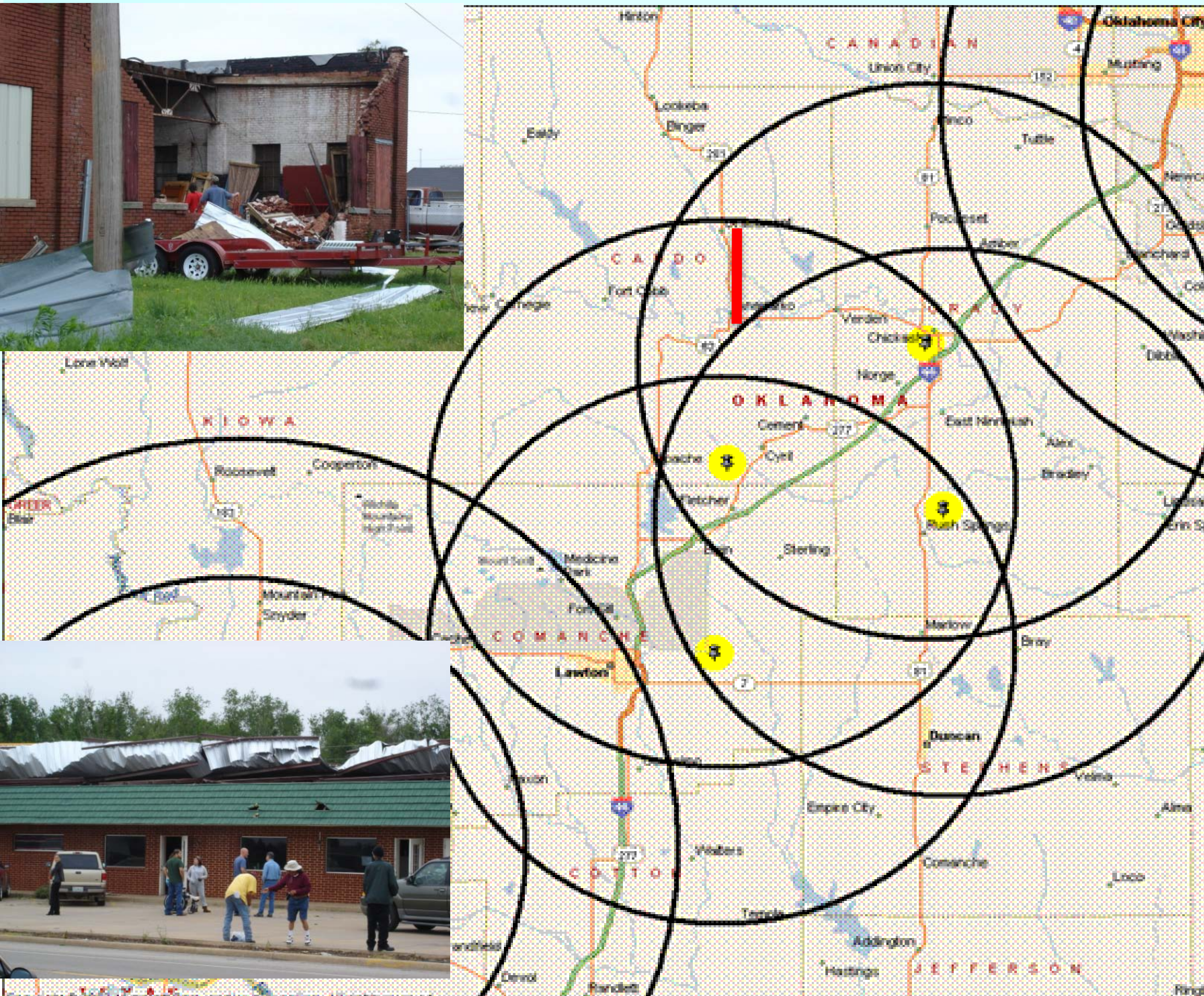

EF2 Tornado
~9:22 – 9:40PM

Prolonged Damaging Winds 100mph+

3 injuries
$43 million+ in property damage

CASA Tornado Warning 9:21

NWS Tornado Warning 9:24

IP1 Radar Network Dual-Doppler Tornado Observation: 2009-May-14

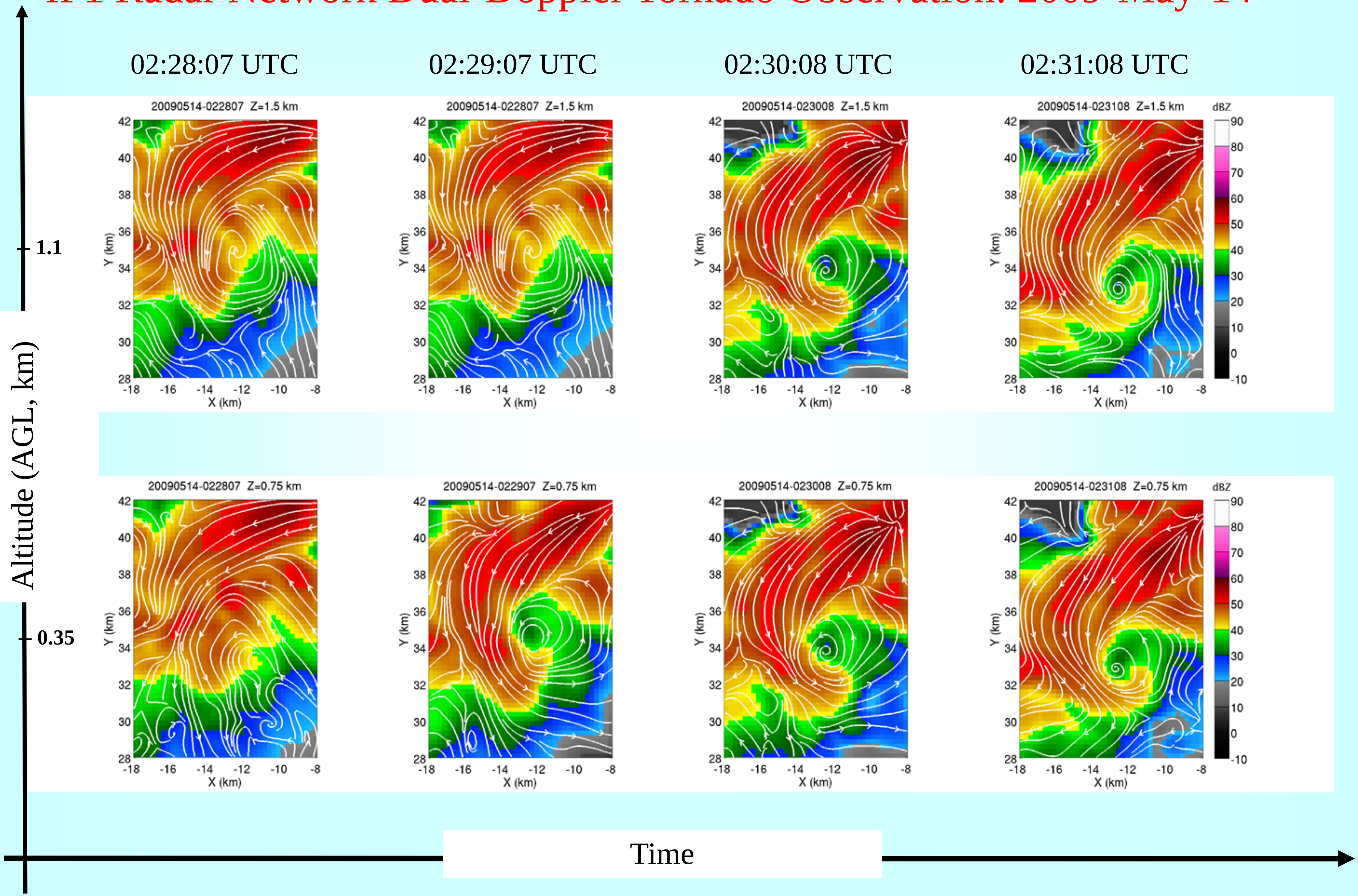

IP1 Radar Network Dual-Doppler Tornado Observation: 2009-May-14

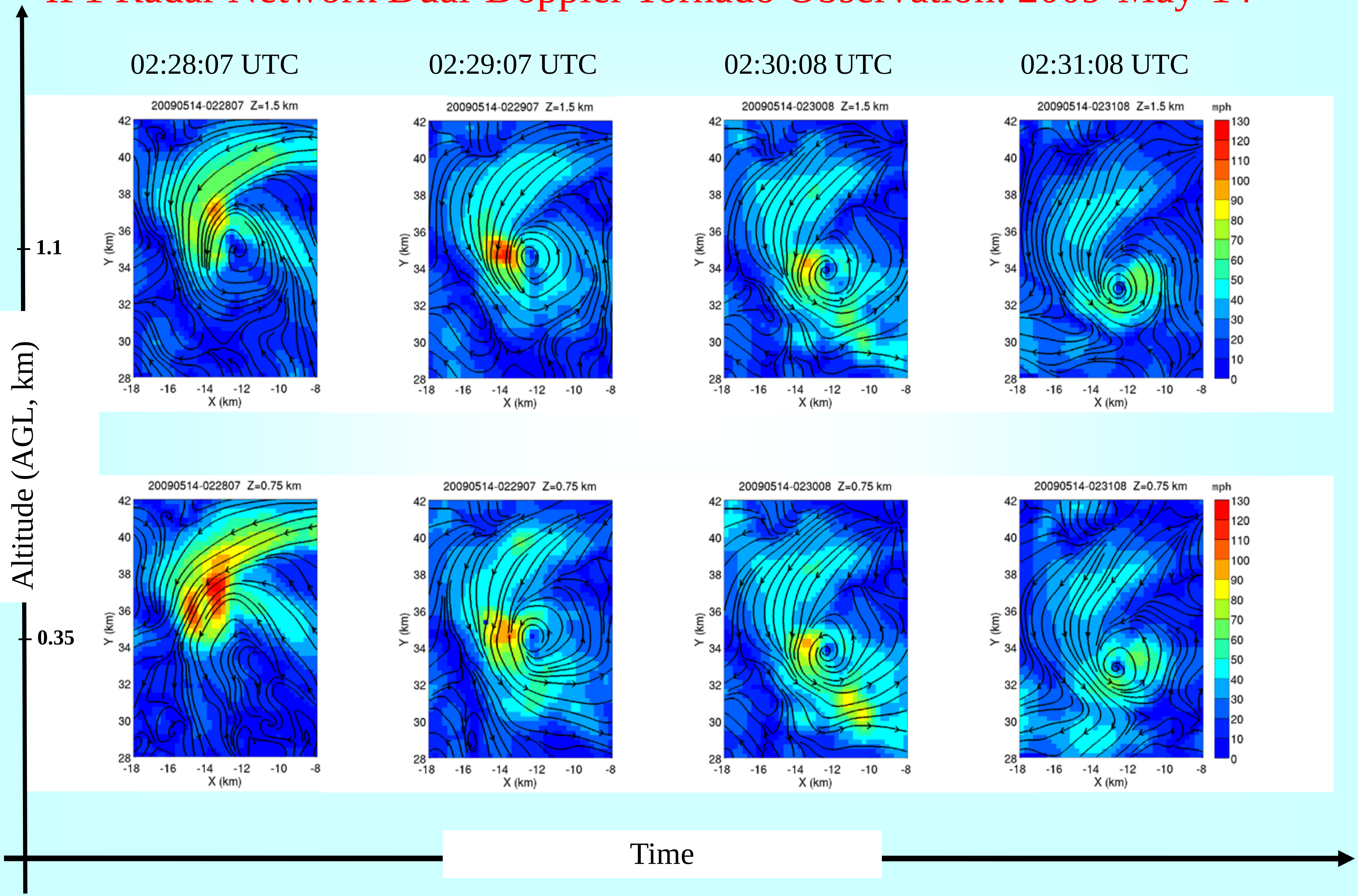

IP1 Radar Network Dual-Doppler Tornado Observation: 2009-May-14
Drop in co-polar correlation due to debris

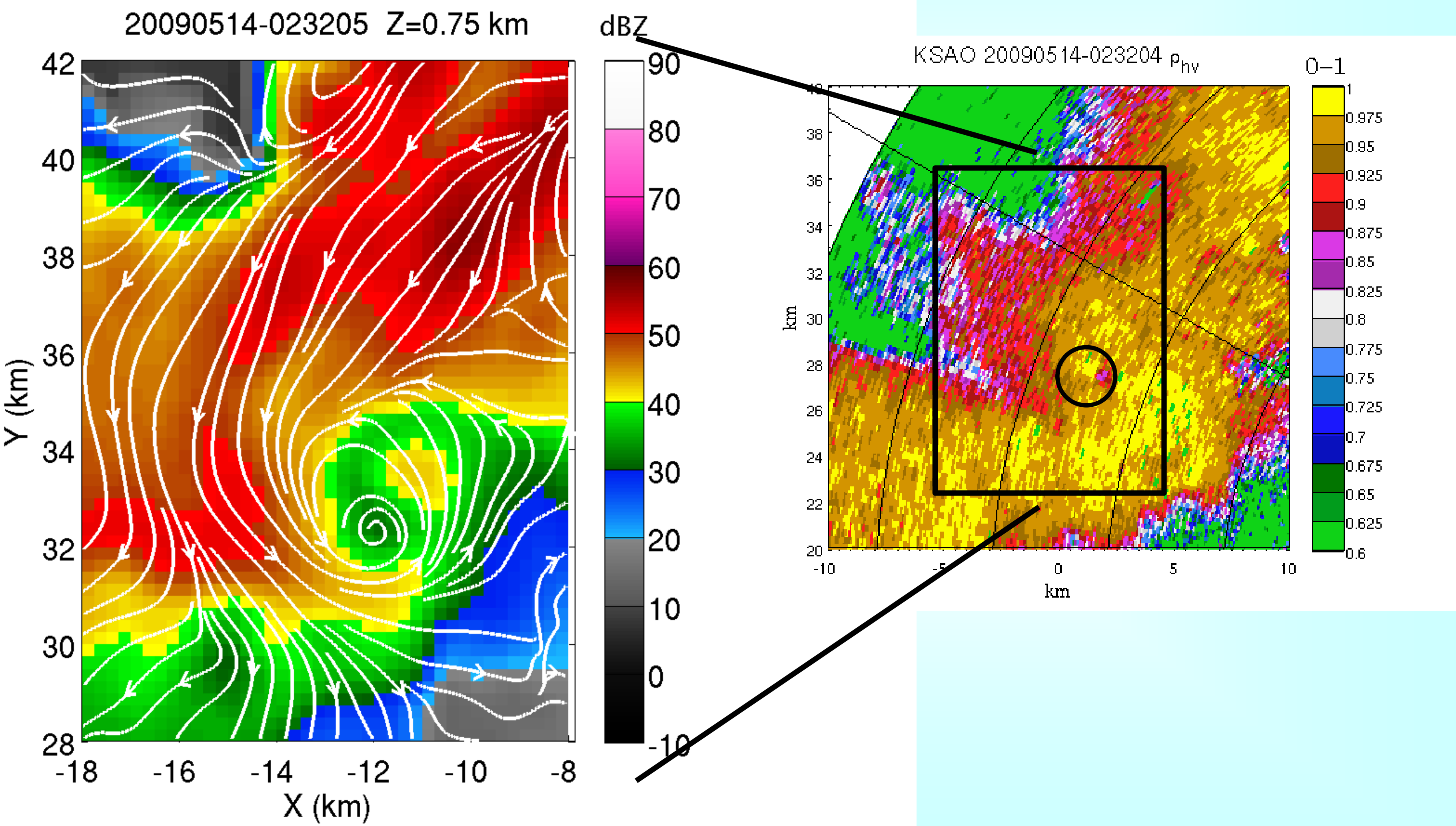

Retrievals Products that are fairly stable and can be considered operationally viable

- Quantitative Precipitation Estimation (2D)
- Drop Size Distribution (Quasi 3D)
- Water content (2 D)
- Hydrometeor Classification (3 D)
- Dual –Doppler based products such as Vorticity (2 D)

Quality of all these products depends on the quality of in-line processing

Thank you